Available online at www.sciencedirect.com

ScienceDirect

Geochimica et Cosmochimica Acta 297 (2021) 288–307

Geochimica et Cosmochimica Acta

www.elsevier.com/locate/gca

Amino acid $\delta^{13}C$ and $\delta^{15}N$ patterns from sediment trap time series and deep-sea corals: Implications for biogeochemical and ecological reconstructions in paleoarchives

Yuan Shen [a,b,*], Thomas P. Guilderson [b,c], Owen A. Sherwood [b,d], Carmen G. Castro [e], Francisco P. Chavez [f], Matthew D. McCarthy [b]

[a] *State Key Laboratory of Marine Environmental Science & College of Ocean and Earth Sciences, Xiamen University, Xiamen, Fujian 361102, China*

[b] *Ocean Sciences Department, University of California, Santa Cruz, 1156 High Street, Santa Cruz, CA 95064, USA*

[c] *Lawrence Livermore National Laboratory, Livermore, CA 94550, USA*

[d] *Department of Earth Sciences, Dalhousie University, Halifax, Nova Scotia B3H 4R2, Canada*

[e] *CSIC, Instituto de Investigaciones Marinas (IIM), Eduardo Cabello 6, 36208 Vigo, Spain*

[f] *Monterey Bay Aquarium Research Institute, Moss Landing, CA 95039, USA*

Received 6 September 2019; accepted in revised form 15 December 2020; Available online 24 December 2020

Abstract

Recent work using compound-specific stable isotopes of amino acids (CSI-AA) in proteinaceous deep-sea corals opens a new realm of high-fidelity reconstruction for biogeochemical and ecological changes in the ocean. However, underlying these CSI-AA paleoceanographic applications are a series of fundamental assumptions, which hold first that baseline-proxy AA isotope values fixed at the base of food webs represent integrated $\delta^{13}C$ and $\delta^{15}N$ values of primary production, and second they are unaltered during subsequent export and incorporation from particles into corals. We explored long-term $\delta^{13}C$ and $\delta^{15}N$ CSI-AA data on a sediment trap time series together with contemporaneous, geographically close deep-sea bamboo corals (*Isidella* sp.) in the California margin, directly testing these assumptions for the first time. Our data show that isotope values of essential ($\delta^{13}C_{EAA}$) and source AAs ($\delta^{15}N_{Phe}$) in sinking particles quantitatively track bulk $\delta^{13}C$ and $\delta^{15}N$ values of export production. These CSI-AA baseline proxies varied independently of carbon flux, trophic position ($TP_{CSI\text{-}AA}$) and microbial alteration, suggesting that they were well preserved in the sinking particles consumed by corals. Paired comparisons between sinking particles and corals revealed minor elevations of $\delta^{13}C_{EAA}$ (by ~2‰) and $\delta^{15}N_{Phe}$ (by ~1‰) in available coral specimens. We hypothesize that the difference in $\delta^{13}C_{EAA}$ is due to the geographic offset in $\delta^{13}C$ values of primary production expected between the (more offshore) sediment trap site and (more onshore) coral specimens, whereas the $\delta^{15}N_{Phe}$ offset is likely related to expected minor trophic fractionation. Using empirical models derived from the sediment trap time series, we demonstrate for the first time that CSI-AA in proteinaceous deep-sea corals can reconstruct known bulk $\delta^{15}N$ values of export production, source nitrogen $\delta^{15}N$ values, and exported $TP_{CSI\text{-}AA}$ values with very good fidelity. Together, these findings represent a major advance in our understanding of AA isotope behavior in modern and paleoarchives, and can be used to underpin the rapidly evolving use of CSI-AA-based tools in multiple paleoceanographic studies and archives.

Keywords: Compound-specific stable isotopes of amino acids (CSI-AA); Sediment traps; Deep-sea corals; Bioarchives; Paleoceanography; Monterey Bay

* Corresponding author.
E-mail address: yuanshen@xmu.edu.cn (Y. Shen).

https://doi.org/10.1016/j.gca.2020.12.012
0016-7037/

1. INTRODUCTION

Stable isotopes of carbon ($\delta^{13}C$) and nitrogen ($\delta^{15}N$) are invaluable tools for investigating element sources, biogeochemical processes, and ecological function in modern and ancient ecosystems (Peterson and Fry, 1987; Fry and Sherr, 1989; Post, 2002). The $\delta^{13}C$ and $\delta^{15}N$ values of living organisms and nonliving suspended and sinking particulate organic matter (POM) are commonly used to infer various aspects of modern ocean biogeochemical cycles (Goericke and Fry, 1994; Rau et al., 1998). The isotopic compositions of sinking POM collected in sediment traps enable longer and more continuous monitoring of surface ocean processes on timescales of months to years (Altabet et al., 1999; Dore et al., 2002; Woodworth et al., 2004; Montes et al., 2013), while isotopic analysis of cored marine sediments and other paleo-archives facilitates biogeochemical and ecological reconstructions far beyond the instrumental period, from centuries to millennia (Hayes et al., 1999; Thunell and Kepple, 2004; Galbraith et al., 2013; Batista et al., 2014).

Traditional 'bulk' stable isotope techniques have been used to investigate marine biogeochemical cycles on a spectrum of timescales, but interpreting these data is often not straightforward. One major problem is the difficulty of resolving the environmental or biological variables which underlie change in bulk isotope values. A second is the typically large gap in temporal coverage between modern instrumental records (high resolution but short duration) and sedimentary archives (longer record but typically lower resolution). Recently, two separate lines of scientific progress, the development of compound-specific isotope analysis of amino acids (CSI-AA) and the development of deep-sea corals as bioarchives, have begun to address these issues in both the open ocean and coastal margins.

CSI-AA offers a powerful set of new tracers allowing the direct resolution of many of the intertwined processes underlying the bulk isotopic signals (e.g., Larsen et al., 2009; Ohkouchi et al., 2017). This approach commonly employs two independent analyses ($\delta^{13}C_{AA}$ and $\delta^{15}N_{AA}$) which exploit differences in isotopic fractionation among individual amino acids (AAs) during metabolic processing. Most $\delta^{13}C_{AA}$ applications are tied to a familiar dichotomy of "essential" versus "non-essential" AAs; the former AA group cannot be synthesized by metazoans, and so $\delta^{13}C$ values remain unchanged up food chains (Howland et al., 2003; Jim et al., 2006; McMahon et al., 2010). As a result, the $\delta^{13}C$ values of essential AAs ($\delta^{13}C_{EAA}$) represent a direct proxy for the $\delta^{13}C$ value of primary production at the base of the food web. The application of $\delta^{15}N_{AA}$ is based on a different grouping, the "source" and "trophic" AAs, which fractionate very differently during trophic transfer (Popp et al., 2007). The source AAs (e.g., phenylalanine) undergo little to no ^{15}N enrichment relative to diet during trophic transfer, because metabolic processes do not form or cleave bonds involving nitrogen (Chikaraishi et al., 2007). Therefore, source $\delta^{15}N$ values formed by primary producers are only minimally altered in higher trophic level organisms. By contrast, the "trophic" AAs (e.g., glutamic acid) exchange α-amino nitrogen atoms during metabolism and become significantly ^{15}N-enriched during trophic transfer with predictable enrichment factors (McClelland and Montoya, 2002; Chikaraishi et al., 2009; McMahon and McCarthy, 2016). As such, paired analysis of $\delta^{15}N$ values for source ($\delta^{15}N_{SrcAA}$) and trophic AAs ($\delta^{15}N_{TrAA}$) can resolve the variations of bulk $\delta^{15}N$ values into two specific contributions: source nitrogen (e.g., nitrate vs. N_2) $\delta^{15}N$ shifts and trophic position changes. Complementary but fully independent, $\delta^{13}C_{AA}$ and $\delta^{15}N_{AA}$ analyses in multiple bioarchives are now producing novel insights into biogeochemical and ecological changes in coastal and open oceans (Ruiz-Cooley et al., 2014; Vokhshoori et al., 2014; McMahon and McCarthy, 2016; Ohkouchi et al., 2017; Sabadel et al., 2019).

Long-lived proteinaceous deep-sea corals represent relatively new bioarchives for past ocean conditions (e.g., Thresher et al., 2004; Roark et al., 2009; Prouty et al., 2011; Guilderson et al., 2013). These colonial animals are ubiquitous in the deep-sea wherever hard substrates occur. They derive their skeletal C and N almost uniquely from sinking particles, thereby recording a history of surface ocean processes (Sherwood et al., 2005; Sherwood et al., 2011; Hill et al., 2014; Glynn et al., 2019). The proteinaceous skeletons are slowly deposited in radial growth layers (50–150 μm/yr) for up to hundreds to thousands of years (e.g., Thresher et al., 2004; Roark et al., 2005; Sherwood et al., 2006; Sherwood and Edinger, 2009; Sherwood et al., 2009). Their structural protein is highly resistant to degradation over at least millennial time scales (Sherwood et al., 2006; Ehrlich, 2010; Strzepek et al., 2014; McMahon et al., 2015). As such, isotopic analysis of coral proteinaceous skeletons can provide long-term records of surface ocean processes with near annual resolution.

Only in the last decade have CSI-AA tools been applied to proteinaceous deep-sea coral records. Sherwood et al. (2011) measured the first $\delta^{15}N_{AA}$ values in annually-banded, proteinaceous deep-sea corals of the Northwest Atlantic margin. The resulting 75 year-long time series was able to decouple physical oceanographic variations from ecological changes, demonstrating the potential of new CSI-AA proxy information in resolving a controversy regarding changes in source nitrate versus food webs. Subsequent studies of $\delta^{13}C_{AA}$ and $\delta^{15}N_{AA}$ in deep-sea corals of the subtropical North Pacific Ocean have revealed striking centennial-scale changes in the source of new nitrogen (nitrate versus N_2 fixation) (Sherwood et al., 2014), and shown how plankton community composition varies with climate regime (Sherwood et al., 2014; McMahon et al., 2015). A growing number of paleoceanographic studies have now expanded the application of CSI-AA to other oceanic regions (e.g., Prouty et al., 2014; Schiff et al., 2014; Williams et al., 2017). These results are providing detailed views of past ocean changes in primary production, nitrogen sources, planktonic food web structures, and long-term human impacts on marine ecosystems.

However, despite major progress in deep-sea coral CSI-AA-based paleoceanographic applications, there remain a number of important uncertainties related to this approach. Chief among these is a detailed understanding of the linkage between exported surface production CSI-AA values and those recorded in coral skeletal protein. The working

assumption has been that isotope values incorporated into proteinaceous coral skeletons (i.e., coral's diet) directly represent those in the exported plankton production. The single existing comparison of CSI-AA normalized distributions between corals and laboratory algal cultures seems to support this idea (Schiff et al., 2014). However, this assumption has never been rigorously investigated, nor directly tested in the ocean. In particular on dynamic margins, surface food webs linked to variations in nutrient supply and planktonic community can shift dramatically, and could impact exported CSI-AA records on varying timescales. In addition, possible microbial activity in sinking particles might also impact the preservation of exported CSI-AA values. Finally, the degree of correspondence between averaged "real world" export production and CSI-AA data preserved in drilled coral skeletal bands, based on a direct comparison of coupled sinking POM-coral samples, has never been examined.

The central objective of this study is therefore CSI-AA proxy development in deep-sea proteinaceous corals: to address these basic unknowns, and provide the first direct evaluation of the accuracy of CSI-AA-based paleoceanographic protein coral applications. We analyzed individual $\delta^{13}C_{AA}$ and $\delta^{15}N_{AA}$ values in a deep-sea sediment trap time series (1999–2004), alongside contemporaneous proteinaceous deep-sea bamboo corals (*Isidella* sp.) in Monterey Bay, California. To achieve our central objective of understanding systematics of CSI-AA values between primary production and ultimate preservation in skeletal gorgonin, we sequentially examine: (1) the main factors governing CSI-AA and bulk isotope values in export production, (2) the influence of seasonality and microbial activity on exported CSI-AA values and patterns, and (3) the correspondence between averaged export POM CSI-AA values and those preserved in contemporaneous skeletal layers of deep-sea coral. Finally, we test whether measured CSI-AA data in these corals can directly reconstruct known/measured surface ocean dynamics, including bulk isotope values of export production, source nitrogen history (e.g., nitrate $\delta^{15}N$ values), and surface plankton food chain length. Together these data strongly support that CSI-AA in deep-sea proteinaceous corals is a direct reflection of CSI-AA data in averaged export production, without major seasonal or degradation biases. These results also represent the first data directly relating CSI-AA values and patterns with bulk $\delta^{13}C$ and $\delta^{15}N$ values of export production through multiple seasonal cycles, representing a foundational data set for understanding CSI-AA systematics in marine particles.

2. METHODS

2.1. Study region and sampling procedures

Sampling was conducted in Monterey Bay, a large open embayment on the central coast of California (Fig. 1). This region experiences strong seasonal upwelling and relaxation in response to local wind forcing and interaction with a California Current meander (Rosenfeld et al., 1994). The upwelled water, formed north of Monterey Bay at Pt. Año Nuevo (Rosenfeld et al., 1994), introduces nutrient-rich water into the central Bay during March-July promoting high primary production in spring and summer (1.5–2.5 g C m^{-2} d^{-1}) (Chavez, 1996; Pennington and Chavez, 2000). Spatial and temporal variations in nutrients and currents influence phytoplankton and zooplankton communities (Kudela and Dugdale, 2000; Fawcett and Ward, 2011; Messié and Chavez, 2017) and collectively affect the amount and composition of exported POM (Pilskaln et al., 1996; Castro et al., 2018), which is the main food source for deep-sea corals in Monterey Bay (Hill et al., 2014). High and variable rates of plankton productivity, complex plankton food web structures, and tight pelagic-benthic coupling make Monterey Bay an ideal region for testing the utility and reliability of CSI-AA-based proxies under varying conditions.

Sinking particles were collected at station M2 (36.697°N, 122.378°W; Fig. 1) using an acid-cleaned cone-shaped Honjo Mark VI sediment trap (Honjo and Doherty, 1988). The trap was deployed at 1200 m depth (~500 m above the seafloor) from January 1999 through December 2004. The trap was outfitted with 13 collection cups that contained preservatives (3.0 mM of mercury chloride and >5 g/L of sodium chloride) and rotated every 14 days. There were gaps in the sampling due to technical issues with sediment trap program or trap retrieval. The collection and handling of samples followed the procedures described in Castro et al. (2018). The oven-dried samples were ground in an agate mortar and stored in polyethylene vials or polycarbonate tubes at room temperature in the dark until elemental and isotopic analyses.

Deep-sea corals were collected in Monterey Canyon (36.747°N, 122.022°W) inshore of the M1 mooring station (Fig. 1). Two bamboo coral specimens (*Isidella* sp.), T1104-A2 and T1104-A11, were live-collected in 2007 at depths of 915 m and 835 m using the Monterey Bay Aquarium Research Institute (MBARI) vessel R/V *Western Flyer* and the ROV *Tiburon*. Coral collection methods were previously reported in Schiff et al. (2014). Briefly, polyp and tissue material was separated from skeletons upon collection, and the samples were washed in seawater and rinsed in freshwater prior to air drying. An organic node (6–8 mm thick) was removed from near the basal attachment of each coral skeleton and decarbonated in 10% HCl. Using scalpel and forceps, organic peels (0.4–0.5 mm thick) were dissected and then rinsed in Milli-Q water and dried. Based on bomb-^{14}C dating, the growth rate of *Isidella* in Monterey Bay was estimated to be 0.14 mm/yr (Schiff et al., 2014); thus each peel represents a 3–4-year time window. Below we present data from only the second and third peels from each coral because they represent the best temporal match to the sediment traps data (1999–2004).

2.2. Bulk $\delta^{13}C$ and $\delta^{15}N$ analyses

Sediment trap samples were separated into aliquots for bulk $\delta^{13}C$ and $\delta^{15}N$ analysis. Aliquots for $\delta^{13}C$ analysis were weighed (~5 mg) into silver boats and acidified by immersion in 6–8% sulfurous acid (H_2SO_3) followed by repeated rinses with Milli-Q water and drying at 60°C

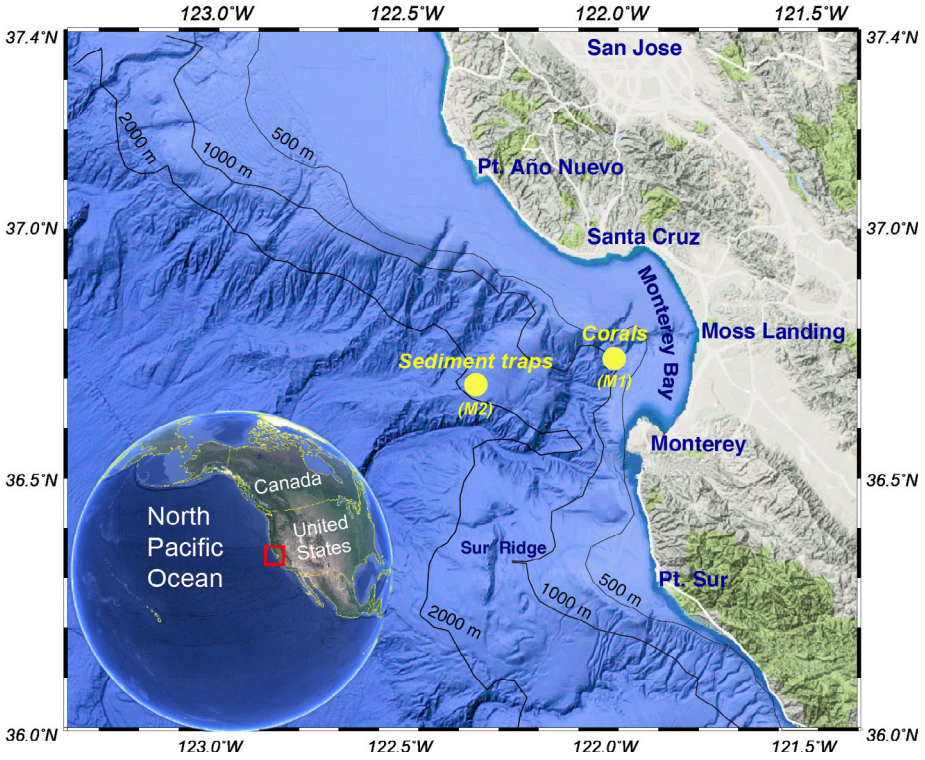

Fig. 1. Study area and sampling locations in Monterey Bay, California. Sediment trap and coral samples were collected at ~1200 m and ~900 m at M2 and M1 mooring stations, respectively.

overnight. The other aliquots for $\delta^{15}N$ analysis (~10 mg) were not pre-treated. Coral peels were acidified during the previous preparation (Section 2.1) and did not undergo any further pre-treatment. Approximately 0.3–0.5 mg of coral peels was used for bulk $\delta^{13}C$ and $\delta^{15}N$. Bulk isotope analysis was performed at the UC Santa Cruz Light Stable Isotope Laboratory using a Carlo Erba 1108 elemental analyzer coupled to Thermo Finnigan Delta Plux XP isotope ratio mass spectrometer following standard procedures (https://websites.pmc.ucsc.edu/~silab/index.php). Isotopic values were corrected for sample size and instrumental drift and were reported in units of per mil (‰) relative to Vienna PeeDee Belemnite (VPDB) and air for $\delta^{13}C$ and $\delta^{15}N$, respectively. Analytical precision as monitored with acetanilide was <0.2‰ for $\delta^{13}C$ and $\delta^{15}N$.

2.3. Amino acid $\delta^{13}C$ and $\delta^{15}N$ analyses

Approximately 15 mg of dried sediment trap and 5 mg of dried coral material was used for amino acid $\delta^{13}C$ ($\delta^{13}C_{AA}$) and $\delta^{15}N$ ($\delta^{15}N_{AA}$) analyses. Hydrolysis, purification, and derivatization followed previously established protocols in batches of 5–7 samples (Silfer et al., 1991; McCarthy et al., 2013; McMahon et al., 2018). An AA mixture of known $\delta^{13}C_{AA}$ and $\delta^{15}N_{AA}$ values and an in-house biological reference standard (homogenized cyanobacteria) was analyzed along with each sample batch. The AA mixture was used to calibrate the $\delta^{13}C_{AA}$ and $\delta^{15}N_{AA}$ results. The cyanobacteria reference, processed in the same way as samples, was used to monitor the consistency of wet chemistry and instrumental analysis (Table EA1). $\delta^{13}C_{AA}$ and $\delta^{15}N_{AA}$ values were determined using a Thermo Trace Ultra gas chromatography (GC) coupled with a Finnigan MAT DeltaPlus XL IRMS at UCSC SIL following chromatographic conditions described in McCarthy et al. (2013) and McMahon et al. (2018). Samples were injected in triplicate, bracketed by triplicate injections of the calibration standard. Final $\delta^{13}C_{AA}$ values were corrected for the added derivatizing reagents following the procedures of Silfer et al. (1991), and final $\delta^{15}N_{AA}$ values were corrected based on the offset between known and measured $\delta^{15}N_{AA}$ values of the calibration standard. The standard deviation of replicate injections for individual AAs in the samples ranged from 0.2‰ to 0.5‰ for $\delta^{13}C_{AA}$ and from 0.1‰ to 0.6‰ for $\delta^{15}N_{AA}$. The relative abundance (mol%) of amino acids was determined from peak areas measured during $\delta^{15}N_{AA}$ analysis. Peak area response factors for individual AAs were calculated from the known-concentration external standards and then applied to sample peak areas to derive molar abundances.

A total of twelve amino acids (AAs) were analyzed for $\delta^{13}C_{AA}$ and $\delta^{15}N_{AA}$, including alanine (Ala), glycine (Gly), threonine (Thr), serine (Ser), valine (Val), leucine (Leu), isoleucine (Ile), proline (Pro), asparagine + aspartic acid (combined as Asx), glutamine + glutamic acid (combined as Glx), phenylalanine (Phe), and lysine (Lys). These AAs were further assigned to several groups based on established classifications (discussed in Section 4.4). For $\delta^{13}C_{AA}$ there are six essential AAs (EAA: Thr, Ile, Val, Phe, Leu, Lys) and six non-essential AAs (NEAA: Gly,

Ser, Asx, Glx, Pro, Ala). For $\delta^{15}N_{AA}$ there are two source AAs (SrcAA: Phe, Lys), seven trophic AAs (TrAA: Glx, Asx, Ala, Leu, Ile, Pro, Val), and three others (Gly, Ser, Thr). Mean $\delta^{13}C_{AA}$ and $\delta^{15}N_{AA}$ values of each group ($\delta^{13}C_{EAA}$, $\delta^{13}C_{NEAA}$, $\delta^{15}N_{SrcAA}$, $\delta^{15}N_{TrAA}$) were calculated as the simple average isotope values of AAs from corresponding groups. To facilitate cross-study comparison, mol%-weighted average was not used here, because mol% values were not routinely estimated by GC-IRMS.

2.4. Parameter calculations

CSI-AA-based trophic position values (TP_{CSI-AA}) of sinking particles were calculated based on the $\delta^{15}N$ values of Glx and Phe following the formulation of Chikaraishi et al. (2009):

$$TP_{CSI-AA} = 1 + (\delta^{15}N_{Glx} - \delta^{15}N_{Phe} - 3.4‰)/7.6‰ \quad (1)$$

where 3.4‰ is the empirical offset between $\delta^{15}N_{Glx}$ and $\delta^{15}N_{Phe}$ determined in aquatic primary producers (cyanobacteria and algae) (McClelland and Montoya, 2002; Chikaraishi et al., 2009) and 7.6‰ is a trophic discrimination factor (TDF) of $\delta^{15}N_{Glx-Phe}$ (Chikaraishi et al., 2009). For detrital material such as sediment trap samples or sediments, this TP_{CSI-AA} value represents the average trophic position of all proteinaceous material sources contained within the sample (McCarthy et al., 2007; Batista et al., 2014). TP_{CSI-AA} values of coral skeletons ($TP_{skeleton}$) represents the trophic position of the coral animal at a given sampling interval, and were calculated based on the skeleton $\delta^{15}N_{Glx}$ and $\delta^{15}N_{Phe}$ values using the following equation:

$$TP_{skeleton} = 1 + [(\delta^{15}N_{Glx} + \partial) - \delta^{15}N_{Phe} - 3.4‰]/7.6‰ \quad (2)$$

where ∂ is a correction factor (3.4‰) proposed by McMahon et al. (2018) to account for a negative $\delta^{15}N_{Glx}$ offset observed in *Isidella* between skeleton and polyp tissue.

Two independent AA-based parameters (DI and ΣV) were calculated to assess the bacterial degradation and resynthesis of organic matter, respectively. The degradation index (DI) was derived from multivariate analysis of mol% of protein AAs following Dauwe et al. (1999):

$$DI = \Sigma[(var_i - AVG_i)/STD_i \times Fact.coef_i] \quad (3)$$

where var_i is the mole % of individual AA_i in our samples and the AVG_i, STD_i and $Fact.coef_i$ are the mean mol%, standard deviation, and factor coefficient of corresponding AA_i from the reference dataset (i.e., Table 1 in Dauwe et al., 1999). More positive DI values are indicative of less biodegradation of organic matter. ΣV, an indicator of microbial resynthesis, is a measure of $\delta^{15}N$ deviation during trophic AA resynthesis and was calculated according to McCarthy et al. (2007):

$$\Sigma V = 1/n\Sigma(|\chi_i - \chi_{mean}|) \quad (4)$$

where n is the number of trophic AAs included in this calculation (Ala, Leu, Ile, Pro, Asx, Glx) and χ_i and χ_{mean} are the $\delta^{15}N$ values of each and the mean of all trophic AAs, respectively. Higher ΣV values are indicative of a greater extent of resynthesis of organic matter.

A number of abbreviations and terminology were used in this study (see Table EA2 for full descriptions). Specifically, 'CSI-AA-based proxies' used below refer to $\delta^{13}C_{Phe}$, $\delta^{13}C_{EAA}$, $\delta^{15}N_{Phe}$, $\delta^{15}N_{SrcAA}$, and TP_{CSI-AA}, the first four of which are further referred to as 'CSI-AA baseline proxies'. The 'baseline' isotope values refer to the source nitrogen (e.g., nitrate or N_2) $\delta^{15}N$ value or/and primary production $\delta^{13}C$ value at the base of the food web.

2.5. Statistical analysis

The coral record has a lower resolution than the sediment trap record. Therefore, the average and standard deviation of bulk and amino acid $\delta^{13}C$ and $\delta^{15}N$ values in the sediment trap time series were flux-weighted so that they are comparable to the coral record. Data used for statistical analysis were checked for normality and homogeneity of variances using Kolmogorov-Smirnov test (two-tailed, $\alpha = 0.05$) and Levene's test (two-tailed, $\alpha = 0.05$), respectively. Significance of group comparison was tested using Mann-Whitney U-test (two-tailed, $\alpha = 0.05$). Relationship between variables and the associated best fit lines were determined using a type II least-squares linear regression. The statistical analyses were performed in SPSS 23.0 (IBM Statistical Package for the Social Sciences Inc.).

3. RESULTS

3.1. Temporal patterns of sinking particles

3.1.1. Organic carbon flux

Particulate organic carbon (POC) flux varied over 25-fold from 5 to 142 mg C m^{-2} d^{-1} over the 6-yr sampling period (Jan 1999–Dec 2004), with maximum flux occurring during the spring and summer upwelling months (Fig. 2; Table 1). The observed temporal pattern and amplitude of carbon flux were comparable to previous sediment trap records in Monterey Bay during non-El Niño years (e.g., Pilskaln et al., 1996).

3.1.2. Bulk and amino acid $\delta^{13}C$ values

Bulk $\delta^{13}C$ values of sinking particles ($\delta^{13}C_{bulk}$) varied ~5‰ from −19.2‰ to −24.0‰ in 1999–2004 (Fig. 2a; Table 1). The flux-weighted average value of $\delta^{13}C_{bulk}$ (−21.5 ± 1.3‰) is consistent with the expected marine origin of sinking particles. Temporal variation of $\delta^{13}C_{bulk}$ roughly followed the trend of carbon flux ($R^2 = 0.345$, $p < 0.01$), i.e., values became more positive from winter into the more productive spring period.

Compound-specific $\delta^{13}C$ values of amino acids differed between the groups of EAA ($\delta^{13}C_{EAA}$) and NEAA ($\delta^{13}C_{NEAA}$). Similar to $\delta^{13}C_{bulk}$, $\delta^{13}C_{EAA}$ varied ~5.0‰ from −18.4‰ to −23.4‰ (flux-weighted avg.: −20.9 ± 1.2‰; Table 1). The $\delta^{13}C_{EAA}$ values closely followed $\delta^{13}C_{bulk}$ throughout the sampling period with minimal offsets (by 0.4 ± 0.7‰) ($R^2 = 0.614$, $p < 0.001$; Figs. 2a, 3b). $\delta^{13}C$ values of Phe ($\delta^{13}C_{Phe}$) also paralleled the changes of $\delta^{13}C_{bulk}$ values, but with a weaker relationship ($R^2 = 0.537$,

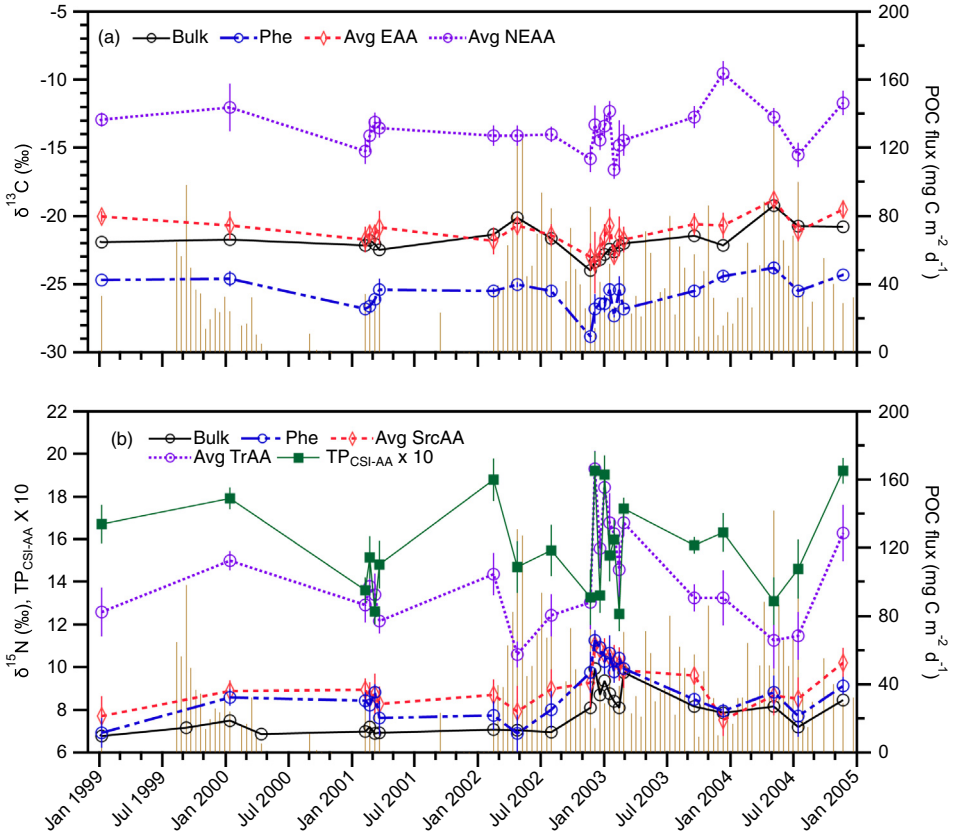

Fig. 2. Temporal patterns of bulk and amino acid $\delta^{13}C$ and $\delta^{15}N$ values in sediment trap samples from January 1999 through December 2004. The vertical brown bar denotes the flux of particulate organic carbon (POC) during the sampling period, and the gaps represent missing sampling due to technical issues. Avg EAA and avg NEAA refer to the simple average (not mol%-weighted) $\delta^{13}C$ values of the six essential AAs (Thr, Ile, Val, Phe, Leu, Lys) and six non-essential AAs (Gly, Ser, Asx, Glx, Pro, Ala), respectively. Avg SrcAA and avg TrAA are the simple average (not mol%-weighted) $\delta^{15}N$ values of the two most reliable source AAs (Phe and Lys; see Section 4.4.1) and seven trophic AAs (TrAA: Glx, Asx, Ala, Leu, Ile, Pro, Val), respectively.

$p < 0.001$) and a larger offset (by 4.2 ± 0.7‰) (Figs. 2a, 3a). Compared to $\delta^{13}C_{EAA}$, $\delta^{13}C_{NEAA}$ values were more enriched (by 6–11‰) and more variable (from −9.5‰ to −16.6‰; flux-weighted avg.: -13.7 ± 1.4‰; Fig. 2a; Table 1). No significant relationship was found between $\delta^{13}C_{NEAA}$ and $\delta^{13}C_{bulk}$ ($R^2 = 0.1$, $p > 0.2$) or carbon flux ($R^2 = 0.05$, $p > 0.2$).

3.1.3. Bulk and amino acid $\delta^{15}N$ values

Bulk $\delta^{15}N$ values of sinking particles ($\delta^{15}N_{bulk}$) ranged from 6.8‰ to 10.0‰ with a flux-weighted average value of 7.8 ± 0.9‰ (Table 2). Slightly higher $\delta^{15}N_{bulk}$ values (e.g., >9‰) were observed mostly during fall and winter periods (Fig. 2b; Table 2). Consistent with previous observations (Altabet et al., 1999), the $\delta^{15}N_{bulk}$ values were not related to carbon flux ($R^2 = 0.0$, $p > 0.5$) or $\delta^{13}C_{bulk}$ values ($R^2 = 0.1$, $p > 0.1$).

The $\delta^{15}N$ values of Phe ($\delta^{15}N_{Phe}$), the most commonly used AA proxy for source nitrogen $\delta^{15}N$ value, varied ~4‰ from 6.9‰ to 11.3‰ with a flux-weighted average value of 8.7 ± 1.2‰ (Table 2). The mean source AA $\delta^{15}N$ values ($\delta^{15}N_{SrcAA}$) varied ~3‰ from 7.5‰ to 11.0‰, with a flux-weighted average of 9.1 ± 0.9‰ (Table 2). The $\delta^{15}N_{Phe}$ values closely followed $\delta^{15}N_{bulk}$ values ($R^2 = 0.703$, $p < 0.001$; Fig. 3c) with small offsets (by 0.9 ± 0.7‰). Values of $\delta^{15}N_{SrcAA}$, also followed those of $\delta^{15}N_{bulk}$, but with a weaker relationship ($R^2 = 0.643$, $p < 0.001$; Fig. 3d) and a larger offset (by 1.2 ± 0.6‰). In comparison, $\delta^{15}N$ values of trophic AAs ($\delta^{15}N_{TrAA}$) were more variable (from 10.6‰ to 19.3‰; flux-weighted avg.: 13.4 ± 2.2‰) and on average ~5‰ more enriched than the $\delta^{15}N_{SrcAA}$ or $\delta^{15}N_{Phe}$ values (Fig. 2b; Table 2).

3.1.4. $TP_{CSI\text{-}AA}$, DI, and ΣV

The $TP_{CSI\text{-}AA}$ values in sinking particles were consistently greater than 1.0, varying from 1.3 to 1.9 with a flux-weighted average value of 1.5 ± 0.2 (Table 2). $TP_{CSI\text{-}AA}$ values were mostly below 1.5 during spring and summer (March–August) and then fluctuated and peaked during fall and winter (Fig. 2b; Table 2). No significant relationships were found between $TP_{CSI\text{-}AA}$ and $\delta^{13}C_{bulk}$ ($R^2 = 0.0$, $p > 0.1$) or $\delta^{15}N_{bulk}$ values ($R^2 = 0.14$, $p > 0.1$). Values of DI and ΣV varied from −0.5 to 0.9 (flux-weighted avg.: 0.3 ± 0.4), and from 0.9 to 2.2 (flux-weighted avg.: 1.7 ± 0.3), respectively, and displayed no temporal patterns (Table 2). There were no strong relationships among $TP_{CSI\text{-}AA}$, DI, and ΣV parameters ($TP_{CSI\text{-}AA}$ vs. DI:

Table 1
Bulk and amino acid $\delta^{13}C$ records (average ± standard deviation) in deep-sea sediment traps (S2) and coral skeletons (T1104_A2 and T1104_A11) in Monterey Bay, California.

Samples	Collection date		POC flux	$\delta^{13}C_{bulk}$	Essential AA $\delta^{13}C$ (‰)						Non-essential AA $\delta^{13}C$ (‰)						$\delta^{13}C_{EAA^1}$	$\delta^{13}C_{EAA^2}$	$\delta^{13}C_{NEAA}$
	Initial	Final	mgC m^{-2} d^{-1}	‰	Thr	Ile	Val	Phe	Leu	Lys	Gly	Ser	Asx	Glx	Pro	Ala	‰		
S2_2-10	12/30/98	1/13/99	33.1	−21.9	−7.7 ± 0.1	−17.4 ± 0.3	−25.9 ± 0.1	−24.7 ± 0.1	−25.2 ± 0.1	−19.3 ± 0.1	−9.3 ± 0.2	−2.1 ± 0.3	−15.3 ± 0.1	−17.2 ± 0.2	−17.2 ± 0.2	−16.5 ± 0.2	−20.0 ± 0.4	−18.9 ± 0.4	−12.9 ± 0.5
S2_4-3	9/1/99	9/15/99	98.4	nd	−12.5 ± 0.2	−17.1 ± 0.1	−23.1 ± 0.3	−23.5 ± 0.2	−23.7 ± 0.2	−17.6 ± 0.2	−9.1 ± 0.1	−6.0 ± 0.7	−13.8 ± 0.2	−13.7 ± 0.1	−14.6 ± 0.4	−14.0 ± 0.3	−19.6 ± 0.5	−18.9 ± 0.4	−11.9 ± 0.8
S2_4-12	1/5/00	1/19/00	23.9	−21.7	−11.3 ± 0.5	−17.8 ± 0.5	−26.2 ± 0.3	−24.6 ± 0.6	−25.5 ± 0.3	−18.9 ± 0.3	−8.6 ± 0.2	0.1 ± 1.1	−13.5 ± 0.7	−16.0 ± 1.0	−16.3 ± 0.5	−17.8 ± 0.1	−20.7 ± 1.0	−19.6 ± 1.0	−12.0 ± 1.8
S2_5-5	4/5/00	4/19/00	5.4	nd	−10.9 ± 0.4	−15.0 ± 0.4	−22.4 ± 0.3	−23.1 ± 0.6	−22.9 ± 0.0	−16.3 ± 0.3	−12.7 ± 0.2	−1.0 ± 0.1	−11.6 ± 0.2	−13.7 ± 0.3	−15.7 ± 0.4	−13.2 ± 0.1	−18.4 ± 0.9	−17.7 ± 0.9	−11.3 ± 0.6
S2_7-13	1/31/01	2/14/01	34.2	−22.1	−13.6 ± 0.3	−19.8 ± 0.3	−26.1 ± 0.4	−26.8 ± 0.2	−26.5 ± 0.2	−17.6 ± 0.7	−11.0 ± 0.1	−7.3 ± 0.3	−15.6 ± 0.3	−17.1 ± 0.1	−23.6 ± 0.6	−16.5 ± 0.6	−21.7 ± 0.9	−20.8 ± 0.8	−15.2 ± 0.9
S2_7-12	2/14/01	2/28/01	30.1	−21.8	−11.9 ± 0.4	−19.3 ± 0.2	−25.1 ± 0.1	−26.6 ± 0.1	−26.3 ± 0.3	−18.4 ± 0.0	−10.1 ± 0.2	−5.2 ± 0.3	−14.9 ± 0.3	−15.8 ± 0.4	−22.3 ± 0.9	−16.5 ± 0.6	−21.3 ± 0.6	−20.5 ± 0.5	−14.1 ± 1.2
S2_7-11	2/28/01	3/14/01	24.7	−22.0	−12.5 ± 0.5	−20.0 ± 0.1	−26.3 ± 0.3	−26.1 ± 0.2	−24.9 ± 0.1	−17.9 ± 0.2	−9.7 ± 0.3	−4.8 ± 0.4	−14.5 ± 0.2	−16.9 ± 0.4	−19.2 ± 0.2	−13.6 ± 0.3	−21.3 ± 0.7	−20.3 ± 0.6	−13.1 ± 0.7
S2_7-10	3/14/01	3/28/01	35.2	−22.4	−10.6 ± 0.7	−18.4 ± 0.4	−25.4 ± 0.4	−25.4 ± 0.8	−25.1 ± 0.2	−20.2 ± 0.3	−12.0 ± 0.1	−0.7 ± 0.3	−14.8 ± 0.3	−18.4 ± 0.2	−17.8 ± 0.2	−17.5 ± 0.5	−20.8 ± 1.2	−19.9 ± 1.2	−13.5 ± 0.7
S2_9-1	2/8/02	2/20/02	38.1	−21.4	−15.2 ± 0.5	−17.7 ± 0.2	−29.0 ± 0.6	−25.5 ± 0.2	−25.3 ± 0.5	−18.1 ± 0.2	−10.7 ± 0.2	−8.2 ± 0.3	−13.9 ± 0.2	−18.1 ± 0.3	−20.2 ± 0.1	−13.3 ± 0.5	−21.8 ± 1.0	−20.4 ± 0.8	−14.1 ± 0.8
S2_9-6	4/17/02	5/1/02	131.2	−20.1	−12.8 ± 0.4	−16.7 ± 0.2	−28.6 ± 0.3	−25.0 ± 0.2	−24.1 ± 0.2	−17.1 ± 0.4	−12.4 ± 0.3	−6.1 ± 0.4	−12.3 ± 0.2	−18.5 ± 0.3	−19.9 ± 0.3	−15.3 ± 0.1	−20.7 ± 0.7	−19.1 ± 0.7	−14.1 ± 0.8
S2_9-13	7/24/02	8/7/02	84.7	−21.6	−11.0 ± 0.4	−17.7 ± 0.3	−29.9 ± 0.3	−25.5 ± 0.4	−26.0 ± 0.3	−18.3 ± 0.3	−11.5 ± 0.2	−3.9 ± 0.3	−12.9 ± 0.1	−18.7 ± 0.2	−20.3 ± 0.0	−16.8 ± 0.3	−21.4 ± 0.8	−19.7 ± 0.8	−14.0 ± 0.6
S2_10-6	11/13/02	11/27/02	85.4	−24.0	−9.7 ± 0.3	−21.9 ± 0.3	−28.0 ± 0.8	−28.8 ± 0.3	−30.4 ± 0.2	−19.5 ± 0.2	−10.5 ± 0.3	−10.4 ± 0.7	−18.4 ± 0.1	−18.1 ± 0.4	−18.9 ± 0.3	−18.3 ± 0.3	−23.0 ± 1.0	−22.0 ± 0.6	−15.8 ± 1.0
S2_10-7	11/27/02	12/11/02	14.3	−23.4	−11.0 ± 0.8	−22.0 ± 0.5	−33.2 ± 1.7	−26.8 ± 1.1	−28.1 ± 0.4	−19.4 ± 0.1	−9.1 ± 0.2	3.9 ± 0.4	−19.9 ± 0.4	−16.9 ± 1.1	−20.8 ± 0.5	−17.1 ± 0.2	−23.4 ± 2.3	−21.5 ± 1.5	−13.3 ± 1.4
S2_10-8	12/11/02	12/25/02	41.3	−23.1	−12.4 ± 0.5	−20.8 ± 0.1	−30.4 ± 0.8	−26.4 ± 0.3	−27.2 ± 0.4	−18.5 ± 0.2	−12.1 ± 0.2	−1.9 ± 0.3	−18.0 ± 0.2	−18.4 ± 0.2	−19.2 ± 0.5	−16.8 ± 0.2	−22.6 ± 1.1	−21.1 ± 0.7	−14.4 ± 0.7
S2_10-9	12/25/02	1/8/03	29.1	−22.8	−11.1 ± 0.1	−19.5 ± 0.2	−26.3 ± 0.2	−26.4 ± 0.6	−26.1 ± 0.5	−19.3 ± 0.3	−10.5 ± 0.1	−3.2 ± 0.6	−16.8 ± 0.2	−17.0 ± 0.2	−16.7 ± 0.3	−16.0 ± 0.4	−21.5 ± 0.9	−20.5 ± 0.9	−13.4 ± 0.8
S2_10-10	1/8/03	1/22/03	51.9	−22.4	−8.4 ± 0.3	−18.3 ± 0.8	−27.8 ± 0.6	−25.4 ± 0.5	−24.8 ± 0.1	−19.7 ± 0.0	−11.4 ± 0.4	−0.9 ± 0.1	−15.6 ± 0.1	−16.6 ± 0.2	−18.3 ± 0.2	−11.4 ± 0.5	−20.7 ± 1.2	−19.3 ± 1.0	−12.3 ± 0.8
S2_10-11	1/22/03	2/5/03	27.2	−22.6	−11.9 ± 0.3	−21.4 ± 0.1	−27.6 ± 0.2	−27.3 ± 0.1	−27.6 ± 0.2	−21.9 ± 0.1	−13.4 ± 0.3	−5.7 ± 0.2	−18.8 ± 0.2	−19.8 ± 0.2	−20.8 ± 0.3	−21.2 ± 0.3	−22.9 ± 0.5	−22.0 ± 0.4	−16.6 ± 0.7
S2_10-12	2/5/03	2/19/03	39.1	−22.2	−10.6 ± 0.1	−21.0 ± 0.3	−25.6 ± 0.9	−25.4 ± 1.0	−25.8 ± 0.4	−20.9 ± 0.3	−14.2 ± 0.4	−4.2 ± 0.6	−17.9 ± 0.4	−18.6 ± 0.5	−19.7 ± 0.5	−14.2 ± 1.5	−21.5 ± 1.5	−20.7 ± 1.1	−14.8 ± 1.8
S2_10-13	2/19/03	3/5/03	70.7	−22.0	−10.1 ± 0.5	−18.7 ± 0.4	−27.2 ± 0.3	−26.8 ± 0.3	−27.4 ± 0.5	−19.9 ± 0.2	−9.2 ± 0.2	−5.7 ± 0.7	−18.4 ± 0.2	−17.8 ± 0.0	−17.7 ± 0.6	−17.6 ± 0.6	−21.7 ± 0.9	−20.6 ± 0.9	−14.4 ± 1.1
S2_12-1	9/10/03	9/24/03	57.7	−21.4	−13.5 ± 0.1	−16.6 ± 0.1	−24.1 ± 0.4	−25.5 ± 0.4	−25.4 ± 0.5	−18.2 ± 0.0	−9.5 ± 0.2	−6.2 ± 0.5	−14.4 ± 0.4	−15.0 ± 0.3	−15.5 ± 0.3	−15.6 ± 0.2	−20.6 ± 0.8	−19.9 ± 0.7	−12.7 ± 0.8
S2_12-7	12/3/03	12/1703	15.7	−22.1	−11.2 ± 0.3	−17.1 ± 0.6	−24.4 ± 0.5	−24.4 ± 0.3	−24.3 ± 0.3	−23.1 ± 0.1	−5.8 ± 0.5	−1.0 ± 0.3	−11.0 ± 0.5	−12.8 ± 0.4	−14.7 ± 0.2	−11.5 ± 0.3	−20.7 ± 0.9	−20.0 ± 0.8	−9.5 ± 0.9
S2_13-4	4/28/04	5/12/04	141.9	−19.2	−9.4 ± 0.2	−15.2 ± 0.2	−22.6 ± 0.2	−23.8 ± 0.4	−25.9 ± 0.1	−16.1 ± 0.1	−10.1 ± 0.3	−3.7 ± 0.3	−14.6 ± 0.2	−15.8 ± 0.2	−18.5 ± 0.2	−13.4 ± 0.2	−18.8 ± 0.6	−18.1 ± 0.5	−12.7 ± 0.6
S2_13-9	7/7/04	7/21/04	100.1	−20.7	−13.5 ± 0.5	−17.8 ± 0.3	−23.4 ± 0.3	−25.5 ± 0.3	−27.9 ± 0.1	−18.4 ± 0.2	−12.3 ± 0.5	−8.4 ± 0.3	−16.3 ± 0.4	−15.8 ± 0.3	−22.0 ± 0.2	−17.9 ± 0.5	−21.1 ± 0.8	−20.6 ± 0.7	−15.5 ± 0.9
S2_14-3	11/8/04	12/6/04	28.9	−20.8	−12.3 ± 0.3	−16.9 ± 0.3	−20.5 ± 0.2	−24.3 ± 0.1	−25.6 ± 0.1	−17.6 ± 0.0	−6.6 ± 0.2	−3.2 ± 0.6	−13.7 ± 0.1	−13.1 ± 0.5	−17.8 ± 0.2	−15.6 ± 0.3	−19.5 ± 0.5	−19.3 ± 0.5	−11.7 ± 0.9
Mean†			*51.8*	*−21.5*	*−11.4*	*−18.1*	*−26.2*	*−25.5*	*−26.0*	*−18.4*	*−10.7*	*−5.0*	*−15.2*	*−16.8*	*−18.8*	*−15.7*	*−20.9*	*−19.9*	*−13.7*
Std†			*37.0*	*1.3*	*1.8*	*1.0*	*2.7*	*1.3*	*1.7*	*1.4*	*1.6*	*2.8*	*2.1*	*1.7*	*2.2*	*2.1*	*1.2*	*1.1*	*1.4*
A2_peel 1			nd	nd	−8.9 ± 0.3	−16.3 ± 0.3	−20.4 ± 0.5	−24.6 ± 1.1	−24.1 ± 0.3	−19.7 ± 1.8	nd	−5.4 ± 0.1	−16.5 ± 0.0	−15.1 ± 0.6	−21.6 ± 0.1	−17.4 ± 0.3	−19.0 ± 2.3	−18.7 ± 2.2	−15.2 ± 0.6
A2_peel 2			nd	nd	−8.8	−15.7	−19.8	−24.0	−24.1	−18.6	nd	−5.4	−16.2	−16.5	−21.7	−17.2	−18.5	−18.3	−15.4
A2_peel 3			nd	nd	−9.5 ± 0.2	−17.0 ± 0.1	−21.2 ± 0.5	−25.2 ± 0.1	−24.5 ± 0.2	−18.6 ± 0.3	nd	−6.0 ± 0.1	−16.8 ± 0.2	−16.3 ± 0.2	−22.0 ± 0.1	−17.1 ± 0.0	−19.3 ± 0.7	−19.0 ± 0.5	−15.6 ± 0.3
A11_peel 1			nd	−16.2	−9.7 ± 0.1	−16.5 ± 0.5	−20.8 ± 0.1	−23.8 ± 0.2	−24.8 ± 0.2	−17.8 ± 0.4	nd	−6.8 ± 0.0	−17.1 ± 0.1	−16.0 ± 0.2	−22.2 ± 0.0	−17.1 ± 0.2	−18.9 ± 0.7	−18.5 ± 0.7	−15.8 ± 0.3
A11_peel 2			nd	nd	−8.4 ± 0.1	−16.1 ± 0.1	−20.2 ± 0.1	−23.3 ± 0.0	−24.4 ± 0.0	−18.2 ± 0.5	nd	−6.3 ± 0.1	−16.3 ± 0.2	−15.6 ± 0.3	−21.7 ± 0.1	−16.5 ± 0.1	−18.5 ± 0.6	−18.1 ± 0.6	−15.3 ± 0.4
A11_peel 3			nd	nd	−9.2 ± 0.1	−17.2 ± 0.0	−21.1 ± 0.2	−27.1 ± 0.3	−24.7 ± 0.1	−16.9 ± 0.0	nd	−6.7 ± 0.1	−16.3 ± 0.2	−15.7 ± 0.3	−22.1 ± 0.0	−16.9 ± 0.0	−19.4 ± 0.4	−19.0 ± 0.3	−15.5 ± 0.4

EAA[1]: average $\delta^{13}C$ value of all six essential AAs; EAA[2]: average $\delta^{13}C$ value of essential AAs without Val. NEAA: average $\delta^{13}C$ value of all six non-essential AAs. Mean† and Std† refer to the flux-weighted average and standard deviation values of all sediment trap samples (exception: mean POC flux, which is a simple average). nd: not determined.

Table 2
Bulk and amino acid $\delta^{15}N$ records (average ± standard deviation) in deep-sea sediment traps (S2) and coral skeletons (T1104_A2 and T1104_A11) in Monterey Bay, California.

Samples	Collection date		$\delta^{15}N_{bulk}$	Source AA $\delta^{15}N$ (‰)		Gly	Ser	Trophic AA $\delta^{15}N$ (‰)							Thr	$\delta^{15}N_{SrcAA}$	$\delta^{15}N_{TrAA}$	TP_{CSIAA}	DI	ΣV
	Initial	Final	‰	Phe	Lys	(‰)	(‰)	Glx	Asx	Ala	Leu	Ile	Pro	Val	(‰)	‰				
S2_2-10	12/30/98	1/13/99	6.8	6.9 ± 0.7	8.5 ± 0.6	8.3 ± 0.2	5.6 ± 0.3	15.4 ± 0.2	11.7 ± 0.1	14.4 ± 0.1	10.4 ± 0.9	10.2 ± 0.4	14.1 ± 0.3	11.9 ± 0.5	0.0 ± 0.4	7.7 ± 0.9	12.6 ± 1.1	1.7 ± 0.1	0.2	2.0 ± 0.2
S2_4-3	9/1/99	9/15/99	7.2	nd	nd	nd	nd	nd	nd	nd	nd	nd	nd	nd	nd	nd	nd	nd	nd	nd
S2_4-12	1/5/00	1/19/00	7.5	8.6 ± 0.4	9.2 ± 0.4	8.0 ± 0.2	6.4 ± 0.2	18.0 ± 0.0	12.5 ± 0.0	16.9 ± 0.3	14.3 ± 0.1	13.3 ± 0.2	15.2 ± 0.1	15.0 ± 0.2	−0.2 ± 0.2	8.9 ± 0.5	15.0 ± 0.5	1.8 ± 0.1	0.1	1.7 ± 0.1
S2_5-5	4/5/00	4/19/00	6.9	nd	nd	nd	nd	nd	nd	nd	nd	nd	nd	nd	nd	nd	nd	nd	nd	nd
S2_7-13	1/31/01	2/14/01	7.0	8.5 ± 0.4	9.4 ± 0.4	7.0 ± 0.1	5.2 ± 0.4	14.6 ± .02	11.5 ± 0.1	14.2 ± 0.4	10.6 ± 0.1	11.3 ± 0.3	13.0 ± 0.4	15.3 ± 0.4	2.6 ± 0.2	8.9 ± 0.5	12.9 ± 0.8	1.4 ± 0.1	−0.4	1.4 ± 0.1
S2_7-12	2/14/01	2/28/01	7.2	8.2 ± 0.7	8.9 ± 0.2	6.2 ± 0.2	3.7 ± 0.4	15.6 ± 0.3	11.9 ± 0.2	15.2 ± 0.3	11.0 ± 0.1	12.5 ± 0.6	14.1 ± 0.4	16.4 ± 0.5	1.3 ± 0.1	8.6 ± 0.8	13.8 ± 1.0	1.5 ± 0.1	0.3	1.6 ± 0.2
S2_7-11	2/28/01	3/14/01	6.9	8.8 ± 0.4	8.7 ± 0.9	6.7 ± 0.3	5.1 ± 0.2	14.2 ± 0.2	11.7 ± 0.1	15.3 ± 0.3	11.2 ± 0.2	12.1 ± 0.5	12.8 ± 0.5	16.7 ± 0.5	2.2 ± 0.9	8.7 ± 1.0	13.4 ± 1.0	1.3 ± 0.1	0.1	1.3 ± 0.2
S2_7-10	3/14/01	3/28/01	6.9	7.6 ± 0.8	8.9 ± 0.1	8.1 ± 0.1	5.9 ± 0.1	14.7 ± 0.2	10.6 ± 0.2	14.2 ± 0.1	11.1 ± 0.2	9.5 ± 0.4	13.0 ± 0.1	12.3 ± 0.1	0.4 ± 0.2	8.3 ± 0.8	12.2 ± 0.6	1.5 ± 0.1	0.1	1.8 ± 0.1
S2_9-1	2/8/02	2/20/02	7.1	7.8 ± 0.6	9.7 ± 0.3	7.8 ± 0.1	7.0 ± 0.2	17.9 ± 0.4	12.5 ± 0.1	17.8 ± 0.2	13.8 ± 0.1	12.6 ± 0.8	14.1 ± 0.3	12.2 ± 0.1	−0.9 ± 0.3	8.7 ± 0.7	14.4 ± 1.0	1.9 ± 0.1	0.1	2.0 ± 0.2
S2_9-6	4/17/02	5/1/02	7.1	6.9 ± 0.9	8.9 ± 0.8	8.3 ± 0.1	5.4 ± 0.1	13.9 ± 0.1	9.7 ± 0.1	12.5 ± 0.3	9.2 ± 0.2	6.6 ± 0.3	12.2 ± 0.3	10.2 ± 0.2	1.5 ± 0.4	7.9 ± 1.2	10.6 ± 0.6	1.5 ± 0.1	0.2	2.2 ± 0.1
S2_9-13	7/24/02	8/7/02	7.0	8.0 ± 0.9	10.0 ± 0.3	8.7 ± 0.1	6.6 ± 0.2	15.6 ± 0.1	11.2 ± 0.0	14.3 ± 0.3	12.4 ± 0.2	8.8 ± 0.3	13.0 ± 0.8	11.9 ± 0.2	1.2 ± 0.2	9.0 ± 0.9	12.5 ± 1.0	1.6 ± 0.1	0.1	1.8 ± 0.2
S2_10-6	11/13/02	11/27/02	8.1	9.8 ± 1.0	8.8 ± 0.7	8.1 ± 0.3	7.2 ± 0.2	15.7 ± 0.2	12.8 ± 0.1	14.8 ± 0.6	11.0 ± 0.5	10.6 ± 0.8	13.8 ± 0.3	12.6 ± 0.5	3.7 ± 0.9	9.3 ± 1.2	13.0 ± 1.3	1.3 ± 0.1	0.6	1.6 ± 0.3
S2_10-7	11/27/02	12/11/02	10.0	11.3 ± 0.5	10.8 ± 0.4	9.4 ± 0.1	7.2 ± 0.6	21.7 ± 0.5	17.2 ± 0.3	20.5 ± 0.2	17.2 ± 0.3	17.8 ± 0.3	20.0 ± 0.2	21.0 ± 0.4	−4.0 ± 0.4	11.0 ± 0.6	19.3 ± 0.9	1.9 ± 0.1	−0.5	1.7 ± 0.2
S2_10-8	12/11/02	12/25/02	8.7	10.9 ± 0.4	10.7 ± 0.4	8.3 ± 0.1	6.6 ± 0.3	16.9 ± 0.5	14.2 ± 0.1	16.4 ± 0.1	13.6 ± 0.5	13.8 ± 0.5	15.4 ± 0.1	18.6 ± 0.3	3.1 ± 0.3	10.8 ± 0.5	15.6 ± 0.9	1.3 ± 0.1	−0.1	1.2 ± 0.2
S2_10-9	12/25/02	1/8/03	9.4	10.3 ± 0.6	10.9 ± 0.5	10.2 ± 0.1	8.5 ± 0.3	20.6 ± 0.3	16.3 ± 0.1	19.5 ± 0.2	16.1 ± 0.1	16.6 ± 0.3	20.2 ± 0.1	19.8 ± 0.3	−1.8 ± 0.3	10.6 ± 0.8	18.4 ± 0.5	1.9 ± 0.1	−0.3	1.9 ± 0.1
S2_10-10	1/8/03	1/22/03	8.8	10.7 ± 0.8	10.3 ± 0.5	9.4 ± 0.2	7.1 ± 0.4	18.1 ± 0.4	14.9 ± 0.3	17.5 ± 0.3	15.4 ± 1.0	15.1 ± 0.8	17.7 ± 0.3	19.1 ± 0.1	0.7 ± 0.3	10.5 ± 1.0	16.8 ± 1.4	1.5 ± 0.1	−0.5	1.3 ± 0.3
S2_10-11	1/22/03	2/5/03	8.4	9.8 ± 0.5	10.7 ± 0.6	8.6 ± 0.1	6.4 ± 0.3	17.7 ± 0.5	14.2 ± 0.3	16.7 ± 0.2	14.9 ± 0.3	15.2 ± 0.1	16.4 ± 0.2	18.8 ± 0.1	1.0 ± 0.1	10.3 ± 0.8	16.3 ± 0.7	1.6 ± 0.1	−0.2	1.1 ± 0.1
S2_10-12	2/5/03	2/19/03	8.1	10.4 ± 0.3	9.9 ± 0.7	8.0 ± 0.4	5.8 ± 0.3	15.7 ± 0.5	13.3 ± 0.4	14.5 ± 0.0	12.7 ± 0.6	13.5 ± 0.6	14.8 ± 0.6	17.5 ± 0.3	2.5 ± 0.2	10.2 ± 0.8	14.6 ± 1.3	1.3 ± 0.1	−0.4	0.9 ± 0.3
S2_10-13	2/19/03	3/5/03	9.8	10.0 ± 0.2	9.8 ± 0.8	10.5 ± 0.5	7.7 ± 0.1	19.0 ± 0.3	15.2 ± 0.4	18.6 ± 0.2	15.2 ± 0.4	14.1 ± 0.2	19.2 ± 0.3	16.3 ± 0.2	1.4 ± 0.3	9.9 ± 0.8	16.8 ± 0.6	1.7 ± 0.0	0.5	2.1 ± 0.1
S2_12-1	9/10/03	9/24/03	8.2	8.5 ± 0.3	10.7 ± 0.3	9.3 ± 0.3	6.8 ± 0.7	16.2 ± 0.2	12.5 ± 0.0	14.6 ± 0.1	12.0 ± 0.1	10.2 ± 0.3	13.8 ± 0.1	13.4 ± 0.5	3.2 ± 0.6	9.6 ± 0.4	13.3 ± 0.6	1.6 ± 0.0	0.7	1.7 ± 0.1
S2_12-7	12/3/03	12/17/03	7.9	8.0 ± 0.3	7.1 ± 0.7	8.8 ± 0.2	6.9 ± 1.0	16.2 ± 0.6	12.9 ± 0.2	13.6 ± 0.3	10.8 ± 1.0	12.8 ± 0.4	14.5 ± 0.3	12.0 ± 0.2	2.8 ± 0.3	7.5 ± 0.7	13.2 ± 1.3	1.6 ± 0.1	0.6	1.3 ± 0.3
S2_13-4	4/28/04	5/12/04	8.2	8.8 ± 0.8	8.6 ± 0.5	8.4 ± 0.6	6.4 ± 0.5	14.6 ± 0.2	11.1 ± 0.0	12.2 ± 0.9	9.5 ± 0.8	8.2 ± 0.3	12.3 ± 0.3	10.9 ± 0.1	4.0 ± 0.5	8.7 ± 0.9	11.3 ± 1.3	1.3 ± 0.1	0.9	1.7 ± 0.3
S2_13-9	7/7/04	7/21/04	7.2	7.7 ± 1.0	9.3 ± 0.2	8.4 ± 0.4	6.6 ± 0.5	14.6 ± 0.3	11.1 ± 0.1	12.8 ± 0.5	10.3 ± 0.9	8.0 ± 0.3	12.5 ± 0.1	11.0 ± 0.1	2.2 ± 0.5	8.5 ± 1.0	11.5 ± 1.1	1.5 ± 0.1	0.7	1.7 ± 0.2
S2_14-3	11/8/04	12/6/04	8.5	9.1 ± 0.4	11.3 ± 0.6	11.3 ± 0.4	9.7 ± 0.5	19.5 ± 0.2	14.9 ± 0.3	18.8 ± 0.3	15.7 ± 0.9	12.8 ± 0.6	18.1 ± 0.1	14.3 ± 0.4	1.0 ± 0.7	10.2 ± 0.7	16.3 ± 1.3	1.9 ± 0.1	0.6	2.2 ± 0.2
Mean†			*7.8*	*8.7*	*9.5*	*8.6*	*6.5*	*16.0*	*12.3*	*14.8*	*11.9*	*10.7*	*14.3*	*13.6*	*1.8*	*9.1*	*13.4*	*1.5*	*0.3*	*1.7*
Std†			*0.9*	*1.2*	*0.8*	*1.0*	*1.0*	*1.9*	*1.8*	*2.2*	*2.2*	*2.9*	*2.3*	*3.1*	*1.6*	*0.9*	*2.2*	*0.2*	*0.4*	*0.3*
A2_peel 1			nd	10.7 ± 0.6	11.2 ± 0.2	12.6 ± 0.6	11.9 ± 1.7	21.8 ± 0.4	18.6 ± 0.3	22.2 ± 0.7	21.7 ± 1.7	23.7 ± 1.4	21.6 ± 0.7	24.2 ± 1.1	−14.2 ± 3.4	11.0 ± 0.6	22.0 ± 2.6	2.5 ± 0.1	nd	1.0 ± 0.5
A2_peel 2			nd	9.8 ± 0.9	10.3 ± 0.7	12.6 ± 0.2	13.2 ± 0.9	21.7 ± 0.3	18.4 ± 0.0	22.4 ± 0.4	21.3 ± 0.4	23.2 ± 1.4	21.2 ± 0.1	24.2 ± 0.3	−10.6 ± 1.4	10.0 ± 1.2	21.8 ± 1.6	2.6 ± 0.1	nd	1.1 ± 0.3
A2_peel 3			nd	9.5 ± 1.2	10.9 ± 0.4	12.1 ± 0.1	12.4 ± 1.0	21.3 ± 0.2	17.8 ± 0.1	21.9 ± 0.1	20.9 ± 0.5	22.9 ± 0.3	20.9 ± 0.0	23.8 ± 0.6	−11.6 ± 0.9	10.2 ± 1.3	21.4 ± 0.8	2.6 ± 0.2	nd	1.1 ± 0.1
A11_peel 1			14.5	8.9 ± 0.6	10.4 ± 0.3	11.7 ± 0.5	11.7 ± 1.5	20.5 ± 0.3	17.8 ± 0.8	20.7 ± 0.2	20.0 ± 0.2	22.0 ± 0.5	20.8 ± 0.1	22.4 ± 0.2	−11.6 ± 1.7	9.7 ± 0.6	20.6 ± 1.1	2.5 ± 0.1	nd	0.9 ± 0.2
A11_peel 2			14.9	9.2 ± 0.6	10.7 ± 0.3	11.9 ± 0.3	13.0 ± 0.6	21.3 ± 0.2	18.4 ± 0.3	21.1 ± 0.2	20.9 ± 0.2	22.7 ± 0.3	21.4 ± 0.4	23.3 ± 0.3	−9.9 ± 0.1	9.9 ± 0.7	21.3 ± 0.7	2.6 ± 0.1	nd	0.9 ± 0.1
A11_peel 3			nd	8.8	nd	11.7	10.6	20.8	17.9	20.5	19.5	22.3	20.4	22.3	−11.8	nd	20.5	2.6	nd	1.0

SrcAA and TrAA are average $\delta^{15}N$ values of source and trophic AAs, respectively. Mean† and Std† refer to the flux-weighted average and standard deviation values of all sediment trap samples (exception: mean POC flux, which is a simple average). nd: not determined.

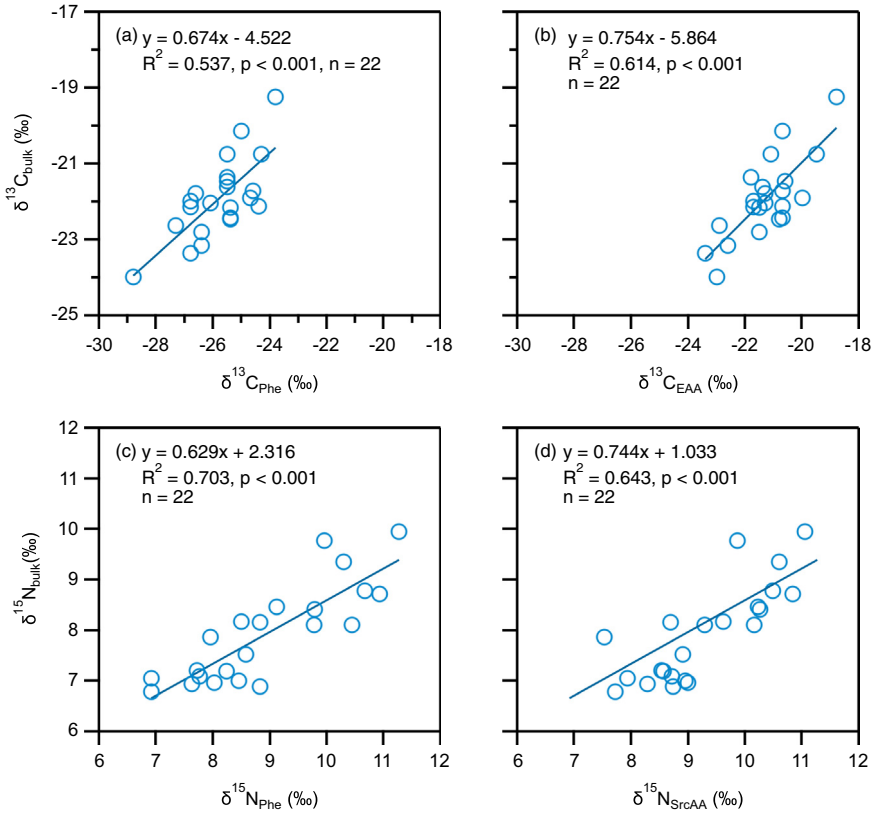

Fig. 3. Relationships between bulk and amino acid $\delta^{13}C$ and $\delta^{15}N$ values in sinking particles. (a) $\delta^{13}C_{bulk}$ vs. $\delta^{13}C_{Phe}$, (b) $\delta^{13}C_{bulk}$ vs. $\delta^{13}C_{EAA}$, (c) $\delta^{15}N_{bulk}$ vs. $\delta^{15}N_{Phe}$, and (d) $\delta^{15}N_{bulk}$ vs. $\delta^{15}N_{SrcAA}$. The blue lines represent the best fit lines (least square method). $\delta^{13}C_{EAA}$: mean $\delta^{13}C$ values of the six essential amino acids; $\delta^{15}N_{SrcAA}$: mean $\delta^{15}N$ value of the two source amino acids (Phe and Lys).

$R^2 = 0.01$, $p > 0.1$; $TP_{CSI\text{-}AA}$ vs. ΣV: $R^2 = 0.31$, $p < 0.05$; DI vs. ΣV: $R^2 = 0.17$, $p > 0.05$).

3.2. Estimation of export production bulk isotope values using sinking particle CSI-AA values

Explicitly, we assume that sinking particles collected in sediment traps are a direct reflection of export production. As noted above, there were strong relationships between $\delta^{13}C_{bulk}$ and $\delta^{13}C_{EAA}$ values in the sediment trap time series (and between $\delta^{15}N_{bulk}$ and $\delta^{15}N_{Phe}$ values; Fig. 3b, c), indicating one can be used to estimate the other. Two empirical models were developed based on the entire data set ($n = 22$):

$$\delta^{13}C_{export\ production}\ (‰) = 0.75 \times \delta^{13}C_{EAA} - 5.9‰ \quad (5)$$

$$\delta^{15}N_{export\ production}\ (‰) = 0.63 \times \delta^{15}N_{Phe} + 2.3‰ \quad (6)$$

The accuracy of these models was evaluated by comparing the measured $\delta^{13}C_{export\ production}$ and $\delta^{15}N_{export\ production}$ values with those estimated using these models (Fig. EA1; Table EA3). The differences between the estimated and measured values represent the errors (or uncertainties) of the empirical models. The errors in the estimates of $\delta^{13}C_{export\ production}$ and $\delta^{15}N_{export\ production}$ using $\delta^{13}C_{EAA}$ and $\delta^{15}N_{Phe}$ were found to be mostly within ±1.0‰ and ±0.5‰, respectively, and they were distributed consistently over the entire range of data (Fig. EA1).

The two equations (5) and (6) were also able to reproduce the observed temporal patterns of $\delta^{13}C_{export\ production}$ and $\delta^{15}N_{export\ production}$ values throughout the 6-yr study period (Fig. 4). The average offsets between the estimated and measured records were relatively small (≤ 1.0‰) and were not significantly different between high and low carbon flux periods (Mann-Whitney U-Test, $p > 0.1$; Fig. EA2). These empirical relationships can potentially be applied to paleoarchives to reconstruct past bulk isotope values of export production using the preserved CSI-AA values (further discussed in Section 4.5).

3.3. Environmental and biological influences on CSI-AA baseline proxies

To evaluate the potential influence of changing productivity, plankton food webs, or particle diagenetic status on CSI-AA baseline proxy values, the time-series sediment trap records of $\delta^{13}C_{EAA}$ and $\delta^{15}N_{Phe}$ (as well as $\delta^{13}C_{Phe}$ and $\delta^{15}N_{SrcAA}$) were regressed against the values of carbon flux, $TP_{CSI\text{-}AA}$, DI and ΣV. The results of the regression analysis revealed no significant relationships in any case examined ($R^2 \leq 0.2$, $p > 0.1$; Fig. 5), indicating that the observed changes in $\delta^{13}C_{EAA}$, $\delta^{13}C_{Phe}$, $\delta^{15}N_{SrcAA}$, and $\delta^{15}N_{Phe}$ values were independent of the variations in carbon flux, trophic transfer, and microbial alteration.

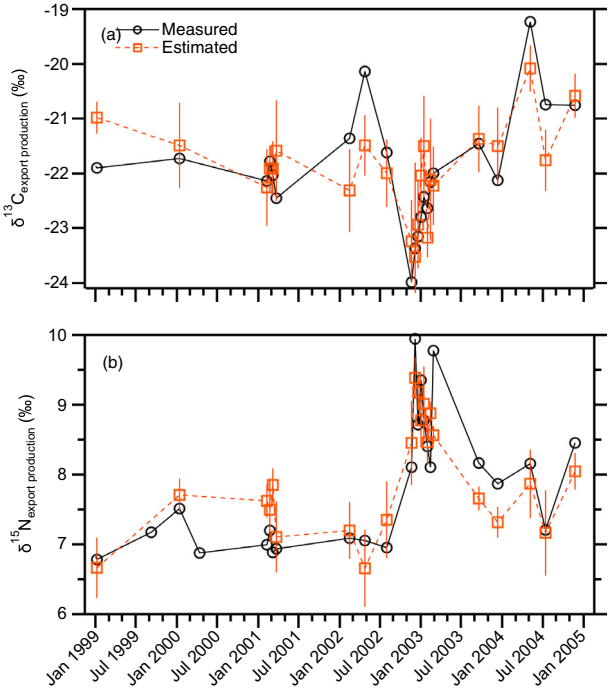

Fig. 4. Temporal variation of measured and estimated $\delta^{13}C_{export\ production}$ and $\delta^{15}N_{export\ production}$ values between January 1999 and December 2004. The measured $\delta^{13}C_{export\ production}$ and $\delta^{15}N_{export\ production}$ refer to the bulk $\delta^{13}C$ and $\delta^{15}N$ values determined in sediment traps. The estimated $\delta^{13}C_{export\ production}$ and $\delta^{15}N_{export\ production}$ values were back calculated from sediment trap $\delta^{13}C_{EAA}$ and $\delta^{15}N_{Phe}$ values using Eqs. (5) and (6), respectively.

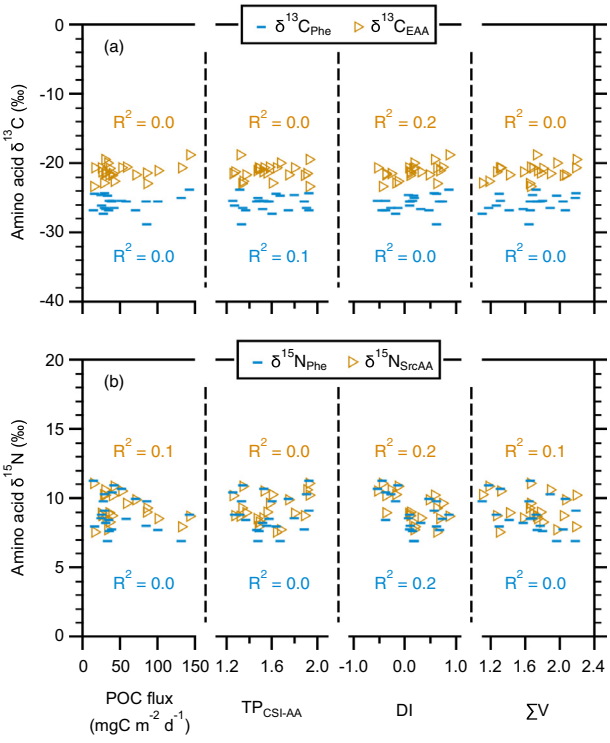

Fig. 5. Isotope values of essential and source AAs plotted against values of particulate organic carbon (POC) flux, trophic position (TP_{CSI-AA}), degradation index (DI), and ΣV. There are two variables on each y-axis (panel a: $\delta^{13}C_{Phe}$ and $\delta^{13}C_{EAA}$; panel b: $\delta^{15}N_{Phe}$ and $\delta^{15}N_{SrcAA}$) and four variables on the x-axis. The coefficient of determination for each regression is labeled as R^2. The p values are not shown and are all greater than 0.1.

3.4. CSI-AA comparisons of sinking particles and deep-sea corals

To evaluate the correspondence of export production and the preserved skeletal CSI-AA data, values of $\delta^{13}C_{AA}$ and $\delta^{15}N_{AA}$ were compared between sediment traps (i.e., sinking particles) and contemporaneous coral outer skeletons (second and third peels) (Fig. 6). In addition, the sediment trap flux-weighted average values of $\delta^{13}C_{AA}$ and $\delta^{15}N_{AA}$ were calculated (Fig. EA3) and subtracted from the mean values in coral skeletons, in order to estimate the mean offsets in $\delta^{13}C_{AA}$ and $\delta^{15}N_{AA}$ values between corals and sinking particles (Fig. 7).

The individual $\delta^{13}C_{AA}$ values in coral skeletons were within the upper range of sinking particle $\delta^{13}C_{AA}$ values (Fig. 6a). The average $\delta^{13}C_{EAA}$ value was slightly more positive in coral skeletons than in sinking particles (by 2.0 ± 1.3‰; Mann-Whitney U-Test, $p < 0.05$; Fig. 7a). However, this offset was largely driven by a large and apparently unique degree of enrichment in the Val $\delta^{13}C$ value (by 5.5 ± 2.8‰). Without Val, the average offset reduced to 1.3 ± 1.2‰ (Fig. 7a). In comparison, the $\delta^{13}C_{NEAA}$ value in corals was slightly depleted (by −1.7 ± 1.4‰; Mann-Whitney U-Test, $p < 0.05$; Fig. 7a). Offsets in individual NEAA $\delta^{13}C$ values varied between +0.8‰ and −3.1‰, and were mostly comparable to the magnitudes of propagated errors (Fig. 7a).

The comparison of individual $\delta^{15}N_{AA}$ values between coral skeletons and the sinking particle data varied strongly by AA groupings (Figs. 6b, 7b). The two source AAs (Phe, Lys; McMahon and McCarthy, 2016) in skeletons showed only small $\delta^{15}N$ offsets relative to sinking particle values (Phe: by 0.6 ± 1.3‰; Lys: by 1.2 ± 0.9‰; Fig. 7b), close to analytical error (Mann-Whitney U-Test, $p > 0.1$). Gly and Ser were termed as "intermediate" AAs in this study (see Section 4.4.2) and they had substantially higher offsets (Gly: by 3.5 ± 1.1‰; Ser: by 5.8 ± 1.6‰; Mann-Whitney U-Test, $p < 0.05$; Fig. 7b). Trophic AAs had by far the largest offsets (by 5-12‰; Mann-Whitney U-Test, $p < 0.05$; Fig. 7b). Finally, a large negative offset was observed for Thr (by −12.8 ± 1.8%; Mann-Whitney U-Test, $p < 0.05$; Fig. 7b). The high trophic AA $\delta^{15}N$ values and low Thr $\delta^{15}N$ values are as expected for animal feeding on POM (McMahon and McCarthy, 2016).

3.5. Reconstructions of surface biogeochemistry and export using coral $\delta^{13}C_{AA}$ and $\delta^{15}N_{AA}$

Based on the empirical models established from our time series sediment traps (Section 3.2), we reconstructed $\delta^{15}N_{bulk}$ values of export production ($\delta^{15}N_{export\ production}$), source nitrogen $\delta^{15}N$ values, and TP_{CSI-AA} values of export production using the coral $\delta^{15}N_{AA}$ records (Fig. 8). As dis-

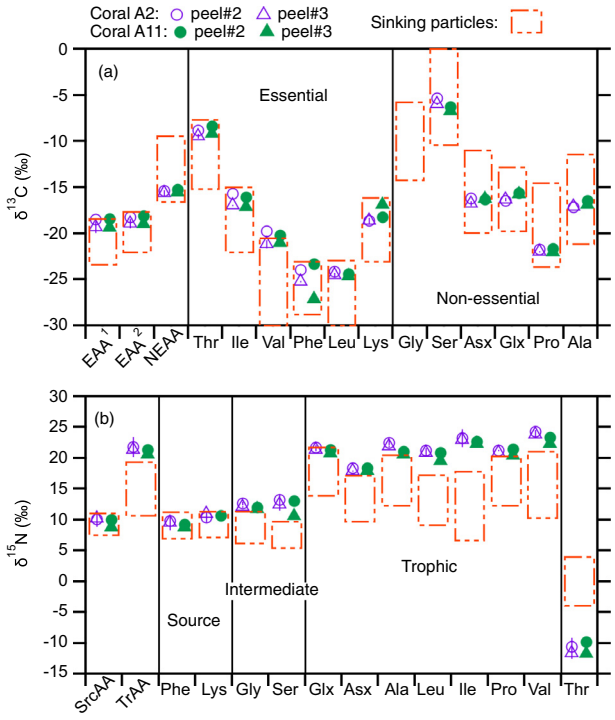

Fig. 6. Comparisons of individual amino acid $\delta^{13}C_{AA}$ and $\delta^{15}N_{AA}$ values between sinking particles and coral skeletons. The dashed box indicates the range of isotope values determined in sinking particle samples (1999–2004). The circle and triangle symbols refer to individual skeletal peels of the two corals. There were three outer skeletal peels sampled from each coral. However, only the second and third peels were included in this comparison, because they best matched the sampling time of sinking particles (see Methods 2.1). EAA^1: average $\delta^{13}C$ value of all six essential AAs; EAA^2: average $\delta^{13}C$ value of essential AAs without Val. $\delta^{13}C$ values for Gly were not determined in the coral samples.

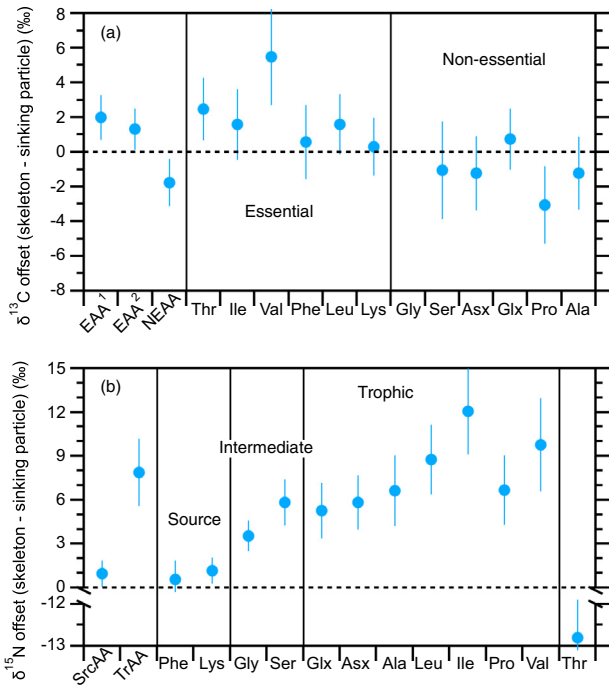

Fig. 7. Mean offsets in individual amino acid $\delta^{13}C_{AA}$ and $\delta^{15}N_{AA}$ values between coral skeletons (average of the second and third peels) and sinking particles (flux-weighted average). Error bars represent propagated standard deviations. EAA^1: average $\delta^{13}C$ value of all six essential AAs; EAA^2: average $\delta^{13}C$ value of essential AAs without Val.

cussed below (Section 4.4.4), a geographic offset in $\delta^{13}C$ primary production values was expected between sites of coral and sediment trap. To avoid this geographical sampling bias, the carbon records were not reconstructed. Such geographic offset was not apparent in source nitrogen $\delta^{15}N$ in Monterey Bay (discussed in Section 4.4.1). In each case of reconstruction, we performed two calculations using the original and the offset-corrected version of $\delta^{15}N_{Phe}$. The corrected version of $\delta^{15}N_{Phe}$ value was calculated by subtracting 0.6‰ from the original $\delta^{15}N_{Phe}$ value to account for the hypothesized small trophic ^{15}N enrichment of Phe in coral skeletons (see Section 4.4.1). The calculated results were then compared with the corresponding reference values to determine the accuracy of the reconstruction. Reference values were obtained from this study and previous multi-year measurements in Monterey Bay (see below).

Average $\delta^{15}N_{export\ production}$ values (8.5 ± 0.3‰) derived from the original coral $\delta^{15}N_{Phe}$ (using Eq. (6)) were similar to the contemporaneous records (7.8 ± 0.9‰, i.e., flux-weighted average $\delta^{15}N_{bulk}$ values of our sediment traps). Correcting for the observed 0.6‰ offset resulted in lower $\delta^{15}N_{export\ production}$ values (7.8 ± 0.3‰), which were almost identical to the reference ranges (Mann-Whitney *U*-Test, $p > 0.1$; Fig. 8a). The source nitrogen $\delta^{15}N$ record was directly inferred from the canonical source AA $\delta^{15}N_{Phe}$ value in corals. The original coral $\delta^{15}N_{Phe}$ values indicated higher source nitrogen $\delta^{15}N$ values (9.3 ± 0.4‰; Fig. 8b) compared to the range suggested by prior work (7.8 ± 0.8‰; i.e., average of prior subsurface nitrate $\delta^{15}N$ values in 1997 and 2002–2004; Altabet et al., 1999; Wankel et al., 2007). However, correcting for the $\delta^{15}N_{Phe}$ offset reproduced more comparable source nitrogen $\delta^{15}N$ values (8.7 ± 0.4‰; Mann-Whitney *U*-Test, $p > 0.1$; Fig. 8b). Finally, the $TP_{CSI\text{-}AA}$ of export production, a measure of the average trophic position of plankton communities that contribute material to the sinking particles, was calculated by subtracting the coral $TP_{skeleton}$ values by one. The coral $TP_{skeleton}$ was estimated based on $\delta^{15}N_{Phe}$ and $\delta^{15}N_{Glx}$ and Eq. (2) (after McMahon et al., 2018). The estimated export production $TP_{CSI\text{-}AA}$ values (~1.6) using either the original or offset-corrected $\delta^{15}N_{Phe}$ values were both within the range of direct $TP_{CSI\text{-}AA}$ measurements in our sediment traps (1.5 ± 0.2) (Mann-Whitney *U*-Test, $p > 0.1$; Fig. 8c).

4. DISCUSSION

4.1. Mechanisms behind varying bulk $\delta^{13}C$ and $\delta^{15}N$ values of export production

The large temporal changes in $\delta^{13}C_{bulk}$ (by ~5‰) and $\delta^{15}N_{bulk}$ values (by ~3‰) of sinking particles could be driven by changes in environmental (e.g., source $\delta^{13}C_{DIC}$ and $\delta^{15}N_{ni-}$

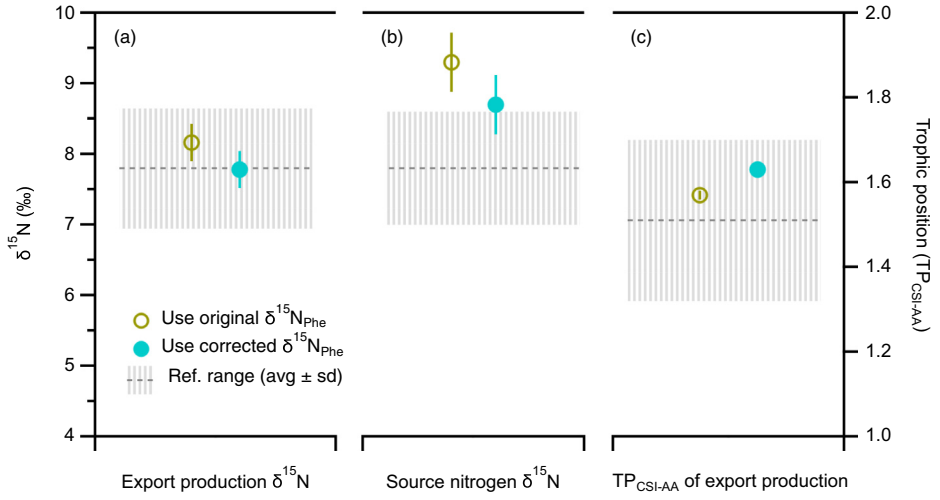

Fig. 8. Reconstructions of (a) bulk $\delta^{15}N$ values of export production, (b) source nitrogen $\delta^{15}N$ values and trophic position ($TP_{CSI\text{-}AA}$) of export production using $\delta^{15}N_{Phe}$ values of coral skeletons (second and third peels, as in Fig. 6). Each calculation was repeated with an offset–corrected $\delta^{15}N_{Phe}$ (minus 0.6‰) to account for the observed small trophic offset between sinking particles and coral skeletons (Fig. 7b). The dashed line and grey shaded area are the average and range (i.e., average ± standard deviation) of reference values. The reference values used for $\delta^{15}N_{export\ production}$ and exported $TP_{CSI\text{-}AA}$ were the flux-weighted average and standard deviation of $\delta^{15}N_{bulk}$ and $TP_{CSI\text{-}AA}$ values measured in our sediment traps (7.8 ± 0.9‰ and 1.5 ± 0.2, respectively). Reference values of source nitrogen $\delta^{15}N$ were the mean and standard deviation (7.8 ± 0.8‰) of prior subsurface nitrate $\delta^{15}N$ values in Monterey Bay [8.0 ± 0.2‰ in 1997 (Altabet et al., 1999) and 7.6 ± 0.8‰ in 2002–2004 (Wankel et al., 2007)]. Error bars represent propagated standard deviations.

$_{trate}$ values) and/or biological (e.g., trophic transfer) processes. The CSI-AA data allow us to explicitly differentiate between these intertwined factors. Understanding to what degree these factors are accurately reflected in amino acids at the molecular level and ultimately recorded in coral CSI-AA data is a key first goal to ground-truthing coral CSI-AA abilities to reconstruct export production isotope values.

For carbon, the sinking particle $\delta^{13}C_{bulk}$ values were strongly related to $\delta^{13}C_{EAA}$ values ($R^2 = 0.614$; Fig. 3b), but not to $TP_{CSI\text{-}AA}$ ($R^2 < 0.1$; Fig. 2b). Given that $\delta^{13}C_{EAA}$ directly trace $\delta^{13}C$ values of primary production, this indicates $\delta^{13}C_{bulk}$ values of export production in Monterey Bay are derived from primary production $\delta^{13}C$ values at the base of the food web and are relatively unaffected by overlying planktonic food web structure. We also observed seasonal variation in sinking particle $\delta^{13}C_{bulk}$ values (i.e., more positive during spring and summer), which generally followed the pattern of previous primary production $\delta^{13}C$ values in Monterey Bay (Fig. 1A in Rau et al., 2001). The seasonal variation in primary production $\delta^{13}C$ values seems not to be driven by the relatively small changes in surface DIC $\delta^{13}C$ values (by <3‰), and instead is more likely related to the highly variable carbon isotopic fractionation during photosynthesis (by 16‰) (Rau et al., 2001). Factors contributing to the variable photosynthetic ^{13}C fractionation in Monterey Bay have not been well resolved and may be in part due to the seasonal supply of trace metal (Rau et al., 2001).

For nitrogen, $\delta^{15}N_{bulk}$ values of export production represent the combined signal of source nitrogen $\delta^{15}N$ values, extent of nitrogen utilization (Rau et al., 1998; Altabet et al., 1999), and potentially a larger impact of trophic alteration. However, as with carbon, the $\delta^{15}N_{bulk}$ values in sinking particles were not related to $TP_{CSI\text{-}AA}$ values ($R^2 < 0.2$; Fig. 2b), but were strongly related to $\delta^{15}N_{Phe}$ values ($R^2 = 0.703$; Fig. 3c). This indicates $\delta^{15}N_{bulk}$ values of export production in Monterey Bay are not strongly influenced by trophic alteration, but instead are primarily set by $\delta^{15}N$ values of source nitrogen and utilization patterns by primary producers. An important nitrogen source for primary production in Monterey Bay is upwelled nitrate occurring during spring/summer (10–20 μM with a $\delta^{15}N_{ni}$-$_{trate}$ range of 6–9‰; Altabet et al., 1999; Wankel et al., 2007; Pennington et al., 2010). In general, $\delta^{15}N$ values of primary production are expected to vary temporally during and after upwelling: upwelling would first lead to production of POM with lower $\delta^{15}N$ values due to partial nitrate utilization and then to elevated POM $\delta^{15}N$ values when most nitrate has been consumed, with the average $\delta^{15}N$ values of POM ultimately reflecting those of upwelled nitrate if utilization is complete (Altabet et al., 1991; Nakatsuka et al., 1992; Altabet et al., 1999). Isotope fractionation associated with partial utilization of surface nitrate in Monterey Bay can be significant, as reflected in the wide-ranging bulk $\delta^{15}N$ values of suspended POM (1–8‰; Rau et al., 1998). Such fractionation is reflected to a lesser extent in the bulk $\delta^{15}N$ values of sinking POM (6–10‰; Altabet et al., 1999; this study).

The impact of these nitrogen isotope dynamics is clearly reflected in our long-term sinking particle $\delta^{15}N_{Phe}$ data. The observed $\delta^{15}N_{Phe}$ range (7–11‰) is a good reflection of contemporaneous subsurface nitrate $\delta^{15}N$ value ranges in this same region (6–9‰; Wankel et al., 2007). Temporally, δ^{15}-N_{Phe} values of sinking particles were lower (e.g., 7–8‰)

during spring and summer and higher (e.g., 9–11‰) during fall and winter (Fig. 2b; Table 2), matching the expected seasonal trends of nitrogen utilization and plankton $\delta^{15}N$ values described above. In addition, we also observed a marked $\delta^{15}N_{Phe}$ elevation (by ~3‰) during the 2002–2003 moderate El Niño period. This isotopic signal is consistent with the limited upwelling and more complete nitrate utilization typical of El Niño conditions, which lead to more positive $\delta^{15}N$ values in the surface nitrogen pool and thereby elevated $\delta^{15}N$ values in phytoplankton and zooplankton biomass (Chavez, 1996; Rau et al., 2003; Décima et al., 2013). Overall, these observations suggest that $\delta^{15}N_{Phe}$ values of sinking particles in this region closely reflect baseline shifts in nitrate $\delta^{15}N$ values, as well as seasonal and longer-term shifts in upwelling dynamics. In turn, this indicates that at least CSI-AA variations in the food source of deep-sea coral archives accurately reflect export production values and source nitrogen history.

4.2. Tracking bulk $\delta^{13}C$ and $\delta^{15}N$ values of export production with sinking particle CSI-AA

Compared to bulk isotope values, both essential and source AAs undergo little to no isotope fractionation during trophic transfer (Chikaraishi et al., 2009; McMahon et al., 2010; McMahon and McCarthy, 2016) and during incorporation into paleoarchives (further discussed in Section 4.4). The strong relationships discussed above between bulk and AA isotope values suggest that empirical models can be used to reconstruct past export production isotope values from the well-preserved CSI-AA baseline proxies (e.g., $\delta^{13}C_{EAA}$, $\delta^{15}N_{Phe}$) in corals or other paleoarchives. Because CSI-AA applications in oceanography and paleoceanography are still in their infancy and almost all ocean organic $\delta^{13}C$ and $\delta^{15}N$ data today are bulk values, until CSI-AA replaces all bulk analyses there is utility in the ability to predict bulk values. However, these CSI-AA proxy values can be used to reconstruct past ocean export production isotope values only if their initial relationships with bulk isotope values are known.

To date, such relationships have not been quantitatively determined, due to very limited paired observations of bulk and AA isotope values in exported POM. Our sediment trap data now demonstrate the $\delta^{13}C_{bulk}$ and $\delta^{15}N_{bulk}$ values of export production can be accurately reproduced from measured $\delta^{13}C_{EAA}$ and $\delta^{15}N_{Phe}$ values, respectively (Figs. 3 and 4; Eqs. (5) and (6)). The uncertainties of the empirical models (C: ±1.0‰; N: ±0.5‰; Fig. EA1) were much smaller than the actual temporal variations in bulk isotope values (C: by ~5‰; N: by ~3‰), suggesting these models can accurately resolve both seasonal and interannual bulk stable isotopic changes in this system. In addition, the uncertainties were very similar during low and high flux extremes (Fig. EA1), suggesting robust performance of the models under varying productivity conditions. These empirical relationships, derived from a long-term record of export production in a highly dynamic coastal system, are the first of their kind and will allow well-grounded quantitative reconstructions of modern and paleo-ocean export production bulk isotope values in similar environments.

4.3. Preservation and fidelity of CSI-AA proxy values in sinking particles

The time series data also allow us to examine the temporal variability of specific CSI-AA-based proxies in sinking particles, and evaluate how different proxies are affected by varying extents of plankton productivity, trophic transfer, and microbial reworking. As noted above, prior studies have shown minimal trophic fractionation of source and essential AAs (McClelland and Montoya, 2002; McCarthy et al., 2007; Chikaraishi et al., 2009; Hannides et al., 2009; McMahon et al., 2010; McCarthy et al., 2013; Batista et al., 2014). However, all such studies were based on limited CSI-AA measurements in short-term culture experiments or discrete field samples.

Our multi-year sediment trap records showed no relationships between CSI-AA baseline proxies (i.e., essential and source AA isotope values) and carbon flux, TP_{CSI-AA}, or the degradation parameters (ΣV and DI) (Fig. 5). The lack of dependence of CSI-AA baseline proxies on carbon flux is important, because it suggests that CSI-AA preserved in paleoarchives are not strongly impacted by past ranges of productivity. It also supports the fundamental CSI-AA assumption that essential and source AA isotope values minimally fractionate during trophic transfers. In contrast to previous work using samples of widely separated trophic levels (e.g., Chikaraishi et al., 2009), our sediment trap time-series resolved fluctuations in TP_{CSI-AA} values at far higher resolution (~0.1 interval on monthly and seasonal time scales). This corroborates the independence of CSI-AA baseline proxies from TP_{CSI-AA} in natural system, and at the same time it suggests TP can be applied in plankton systems at a much finer scale.

4.3.1. Influence of bacterial degradation

In contrast to metazoan trophic transfer, the influence of microbial reworking on AA isotopic fractionation patterns remains only poorly understood. Bacteria attached to sinking particles can produce ectoenzymes to respire and transform POM (Smith et al., 1992; Hansman et al., 2009), potentially altering AA isotopic composition. While different studies have observed different CSI-AA alteration patterns during microbial alteration, the main baseline proxies ($\delta^{13}C_{EAA}$ and $\delta^{15}N_{Phe}$) have so far been observed to retain their isotopic information (McCarthy et al., 2007; Hannides et al., 2013; Steffan et al., 2015; Ohkouchi et al., 2017; Yamaguchi et al., 2017). However, any linkage of microbial degradation to CSI-AA baseline proxy values has never been comprehensively investigated over a large sample set of detrital organic matter.

The two independent AA-based parameters (DI and ΣV) used for our sediment trap time series track separate aspects of microbial alteration. The DI indicates the extent of microbial degradation based on mol% changes of protein AA composition. DI values have been found to decrease from fresh phytoplankton (1–1.5) to refractory sediment organic matter (<−2) (Dauwe et al., 1999). The moderate level of our DI values (flux-weighted average: 0.3 ± 0.4) suggests the sinking particles have been partially degraded during transit to the deep ocean. However, the lack of rela-

tionship between $\delta^{13}C_{EAA}$ (or $\delta^{15}N_{Phe}$) values and DI values suggests negligible impact of microbial degradation on these CSI-AA baseline proxies in sinking particles. This finding contrasts strongly with results on marine suspended particles, which have shown increasing $\delta^{15}N_{AA}$ and $\delta^{13}C_{AA}$ values with depth due to non-selective isotopic enrichment during extracellular enzymatic hydrolysis (Hannides et al., 2013; Yamaguchi et al., 2017). The discrepancy is mirrored in relative bulk isotope changes, and is most likely associated with the relatively rapid settling of sinking particles (16–95 m/day in Monterey Bay) (Shanks and Trent, 1980; Pilskaln et al., 1998) that limits extensive microbial isotopic fractionation.

In contrast to DI, the ΣV parameter indicates the extent of isotope fractionation driven by microbial resynthesis, based on deviations from the approximately universal autotrophic marine algal $\delta^{15}N_{AA}$ pattern (McCarthy et al., 2007; McCarthy et al, 2013). Elevated ΣV values in the organic matter pool indicate microbial addition of resynthesized proteinaceous material (Fogel and Tuross, 1999; McCarthy et al., 2007; Calleja et al., 2013). Some of our sediment trap ΣV values (0.9–2.2) were slightly higher than commonly observed ΣV values in fresh marine plankton (mostly 0.5–1.5) (McCarthy et al., 2007; Hannides et al., 2013; Batista et al., 2014). These values suggest some microbial biomass has been incorporated into sinking particles, consistent with our DI values and prior bacterial biomarkers (D-amino acids) and radiocarbon dating analysis in other oceanic regions (McCarthy et al., 2007; Hansman et al., 2009). However, the lack of correlation between ΣV and $\delta^{13}C_{EAA}$ (or $\delta^{15}N_{Phe}$) aligns with the DI data and suggests modest bacterial alteration has minor impact on CSI-AA baseline proxy values.

4.3.2. Sinking particle TP_{CSI-AA}: tracing planktonic food web structure

The TP_{CSI-AA} is becoming one of the most potentially powerful CSI-AA paleoproxies, which indicate changes in planktonic food web length, typically related to nutrient availability (Batista et al., 2014, Sherwood et al., 2014; Ohkouchi et al., 2017). Our TP_{CSI-AA} data suggest a close correspondence between seasonal changes in surface planktonic food web structure and fine-scale changes in sinking particle TP_{CSI-AA}. The calculated range of TP_{CSI-AA} (1.3–1.9) indicates a mixed planktonic source of sinking particles, consistent with previous microscopic observations of coexisting phytoplankton and zooplankton components in sediment traps (Pilskaln et al., 1996; Beaulieu and Smith, 1998). Seasonally, lower TP_{CSI-AA} values observed in spring and summer (Fig. 2b) suggest shorter planktonic food webs during productive months, likely due to a phytoplankton community shift to larger cells with less grazing. This interpretation is supported by previous field measurements that showed increasing phytoplankton cell size with productivity (Chavez, 1996; Wilkerson et al., 2000). Further, most of the highest TP_{CSI-AA} values were observed during the 2002–2003 moderate El Niño period (Fig. 2b), consistent with a previous zooplankton study that reported enhanced carnivory during El Niño (Décima et al., 2013). Together, these results strongly support the application of TP_{CSI-AA} in corals and other paleoarchives as an indicator of planktonic food web structure, and also suggest that at least in ocean margins small fluctuations of TP_{CSI-AA} (e.g., by ~0.2–0.5) may indicate meaningful change.

4.4. Incorporation of sinking particle CSI-AA values into proteinaceous coral skeletons

A core, yet so far untested, assumption for many CSI-AA paleoceanographic applications is that baseline AA isotope values being recorded in corals match those in their food sources, assumed to be essentially sinking particles (e.g., Sherwood et al., 2005; Hill et al., 2014). Our data allow us to directly examine this assumption and investigate incorporations of other groups of AAs, by taking into account the export dynamics in Monterey Bay. Carbon budget estimates indicate a large fraction of fixed carbon is advected offshore by upwelling filaments prior to vertical sinking as export flux (Pilskaln et al., 1996; Olivieri and Chavez, 2000; Pennington et al., 2010). As a consequence, sinking particles and coral skeletons collected in deep water should integrate isotopic signals from both overlying surface water and adjacent inshore water.

4.4.1. Source AA $\delta^{15}N$ (Phe and Lys)

We observed a close match between sinking particles and coral skeletons in the $\delta^{15}N$ values of the best source AAs, Phe and Lys (Fig. 7b). We note that the traditional source AA grouping includes Gly and Ser (and also Met, which was not measured in this study). However, in contrast to Phe and Lys, the other AAs showed moderate to large ^{15}N enrichments in corals (Fig. 7b). Accumulated literature on $\delta^{15}N_{AA}$ fractionation with trophic transfer has now shown that only Phe, Lys, and Met reliably meet the basic assumption of minimal fractionation with trophic transfers (recently reviewed by McMahon and McCarthy, 2016). Our results are consistent with this expectation, and support a shift in categorization of Phe and Lys as 'true' source AAs.

The small offsets in Phe and Lys $\delta^{15}N$ values between corals and sediment traps are close to the propagated uncertainties (Phe: by 0.6 ± 1.3‰; Lys: by 1.2 ± 0.9‰). However, they could potentially be derived from the small kinetic fractionations expected for a minor metabolic transamination of Phe and an irreversible transamination of Lys, respectively, during trophic transfer (Chikaraishi et al., 2007; Chikaraishi et al., 2009; McMahon and McCarthy, 2016). In fact, our observed offsets for Phe and Lys ^{15}N enrichments are remarkably similar to previous TDF values in the literature (Phe: by 0.4 ± 0.5‰, Lys: by 0.8 ± 1.5‰; Chikaraishi et al., 2009; McMahon and McCarthy, 2016). The small offsets observed in source AA $\delta^{15}N$ values are unlikely related to the geographic difference in sampling locations. In Monterey Bay, nitrate concentrations onshore (near our coral site) are in general higher than those of the offshore sediment trap site (Chavez et al., 2017), suggesting different nutrient and water-mass post-upwelling trajectories. However, prior independent $\delta^{15}N$ measurements for subsurface nitrate in Monterey Bay (Wankel et al., 2007) and for source AAs

in California margin deep-sea bamboo corals have both suggested very similar $\delta^{15}N$ values between nearshore and offshore regions. Overall, the small isotopic offset of source AAs (particularly Phe) in coral skeletons reaffirms the reliability of coral Phe (or/and Lys) as direct proxies for source nitrogen $\delta^{15}N$ values. At the same time, the correspondence to expected trophic offsets also suggests baseline reconstructions might be improved by small trophic corrections (discussed in Section 4.5).

4.4.2. "Intermediate" AA $\delta^{15}N$ (Gly and Ser)

As noted above, Gly and Ser were originally designated as source AAs (Popp et al., 2007) given the low trophic fractionations (<1‰) observed in initial feeding experiments (McClelland and Montoya, 2002). However, accumulated studies in the last decade have consistently shown extremely variable, and often large, trophic fractionations for Gly and Ser mainly in higher level consumers (Germain et al., 2013; Hoen et al., 2014; Nielsen et al., 2015; McMahon and McCarthy, 2016). For these reasons, a recent review on this subject emphasized that Gly and Ser cannot be reliably used as source AAs (McMahon and McCarthy, 2016). Our comparisons between deep-sea corals and their sinking POM food source support this conclusion. We found that Gly and Ser exhibited a trophic enrichment of 4–6‰ in the coral skeletons, a range falling between those of source AAs (by ~1‰) and trophic AAs (by 5–12‰).

The moderate $\delta^{15}N$ fractionations of Gly and Ser are likely associated with their different modes of amino nitrogen transfers compared to other AAs. Compared to the source Phe and Lys, Gly and Ser potentially express higher degrees of isotopic fractionations because Gly and Ser can interconvert with each other via the reversible transamination that involves cleavage of C-N bond (in the presence of enzyme serine-glyoxylate transaminase) (Berg et al., 2002). However, unlike the trophic AAs (e.g., Glx, Asx, Ala, Leu, Ile, etc.), Gly and Ser do not readily exchange amino nitrogen with the heavily fractionated central nitrogen pool, and so would be expected to have lower isotopic fractionations than the traditional "trophic" AA group (O'Connell, 2017). Given the distinct metabolic pathways of Gly and Ser and their intermediate extent of trophic fractionations, we propose a separate classification for Gly and Ser as "intermediate" AAs. This term is in particular appropriate in any study involving higher level consumers.

4.4.3. Trophic AA $\delta^{15}N$ (Glx, Asx, Ala, Leu, Ile, Pro, Val): first TDF values for deep-sea corals

Trophic AAs were all substantially ^{15}N-enriched in coral skeletons compared to sinking particles (by 5–12‰; Fig. 7b), as would be expected for a consumer. The enrichment of nitrogen isotope values from diet to consumer, a key factor commonly known as the trophic discrimination factor (TDF), has never been determined in deep-sea proteinaceous corals. The TDF is an important consideration in assessing the accuracy of $TP_{CSI\text{-}AA}$ values, which are used in corals and other paleoarchives as a proxy for changes in the plankton community (e.g., Batista et al., 2014; Sherwood et al., 2014). Estimation of TDF values typically relies on feeding experiments (McMahon and McCarthy, 2016). However, direct feeding experiments are not currently possible for deep-sea corals because representative genera (*Isidella*, *Gerardia*, etc.) have never been maintained in aquaria, with realistic food sources representing an additional challenge. Therefore, field observations are likely the only realistic way to estimate TDF values for deep-sea corals.

Sinking particles consumed by deep-sea corals are first assimilated by coral polyp tissues (the living coral animal) before being incorporated into the structural protein skeleton. While we do not have data for the living polyps of the corals we analyzed, we were able to calculate the TDF values for deep-sea protein corals by first comparing trophic AA values in sinking POM versus those in the coral skeleton, and then applying recently published polyp-minus-skeleton correction factors (McMahon et al., 2018). McMahon et al. (2018) recently showed that trophic AAs incorporated into protein coral skeletons have a consistent negative 3–4‰ offset compared to the same AAs present in the living coral polyp animal, with very similar offsets observed across three genera and very different ocean regions (including Monterey Bay *Isidella* sp.). We therefore applied McMahon et al.'s correction factors (i.e., skeleton minus polyp tissue) to our coral skeleton data to determine the true TDF values of each AA during the trophic transfer from sinking particles to live coral tissues (referred to as "TDF_{AA}") (Fig. EA4b). Assuming the trophic level of coral polyp is one greater than our flux-weighted average POM, the TDF_{AA} value was calculated:

$$TDF_{AA} = \Delta\delta^{15}N_{(skeleton\text{–}sinking\ particle)} - \Delta\delta^{15}N_{(skeleton\text{–}polyp)} \quad (7)$$

where $\Delta\delta^{15}N_{(skeleton\ -\ sinking\ particle)}$ is the ^{15}N enrichment of a given AA from sinking particle to coral skeleton (as in Fig. 7b) and $\Delta\delta^{15}N_{(skeleton\ -\ polyp)}$ is the previously observed correction factor for individual AA (i.e., skeleton minus polyp; Table 1 in McMahon et al., 2018).

These first TDF_{AA} values for deep-sea proteinaceous corals (Fig. EA4b) showed large ^{15}N enrichments from sinking particles into coral polyps for trophic AAs, ranging from 8.7 ± 1.9‰ in Glx to 15.7 ± 2.9‰ in Ile (mean trophic AAs: 11.4 ± 2.0‰). The TDF value of the canonical trophic AA Glx (i.e., TDF_{Glx}: 8.7 ± 1.9‰; Fig. EA4b) is within the range observed for almost all organisms (McMahon and McCarthy, 2016). Using this TDF_{Glx} value and the TDF_{Phe} value (0.8 ± 1.3‰), we were then able to calculate the trophic-source $TDF_{Glx\text{-}Phe}$ value ($=TDF_{Glx} - TDF_{Phe}$) which is commonly used for most $TP_{CSI\text{-}AA}$ calculations. The mean $TDF_{Glx\text{-}Phe}$ determined from our data for *Isidella* polyp was 7.9‰, essentially identical to the commonly applied 7.6‰ value (McClelland and Montoya, 2002; Chikaraishi et al., 2009), which is now understood to be characteristic of ammonia-excreting primary and secondary consumers (McMahon and McCarthy, 2016). Our results therefore indicate that while for many trophic AAs $\delta^{15}N$ fractionation is very large, the trophic-source $TDF_{Glx\text{-}Phe}$ values calculated in corals are very similar to those in many other taxa. This confirms the use of the standard $TP_{CSI\text{-}AA}$ formulas for coral paleoproxy

applications, as well as supporting the universal nature of correction factors proposed by McMahon et al. (2018).

An unexpected observation, however, was the very large TDF values of several trophic AAs (Ile, Leu, Val, Pro; Fig. EA4b). After correcting for skeleton-to-polyp offsets, these AAs therefore had far greater TDF values (12–16‰; Fig. EA4b) than Glx, a feature not observed across multiple other taxa (McMahon and McCarthy, 2016). These large fractionations were not due to sampling artifacts, because the same pattern was observed in all skeletal layers, and in both corals. We also re-analyzed the previously published trophic AA $\delta^{15}N$ values in *Isidella* polyps and skeletons in Sur Ridge off the California coast (McMahon et al., 2018), and we found that this earlier data contained exactly the same patterns (i.e., greater $\delta^{15}N$ fractionations in Leu, Ile and Val than in Glx). This suggests that these large TDF values for Ile, Leu, Val, and Pro are a consistent feature of deep-sea bamboo corals, and so that previously proposed multi-AA calculations of $TP_{CSI\text{-}AA}$ (e.g., McMahon and McCarthy, 2016; and references therein) likely cannot be used in deep sea corals.

Specific mechanisms behind the extremely large TDF values for these other trophic AAs are not clear. Microbial degradation is not a likely explanation given that the corals were live-collected and had ΣV values (~1.0) even lower than those in sinking particles. One provocative speculation is that there may be additional catabolic pathways for several highly fractionated trophic AAs (e.g., Ile, Leu, and Val) in protein corals, through which lighter ^{14}N is preferentially removed from the metabolic pool. Future labelling studies tracing biochemical transformations of individual AAs in coral tissues will help untangle this riddle.

4.4.4. Essential AA $\delta^{13}C$ (Thr, Ile, Val, Phe, Leu, Lys)

Unlike trophic AA $\delta^{15}N$ values, there are almost no $\delta^{13}C_{EAA}$ offsets between coral skeleton and polyp for this (or other) deep-sea proteinaceous coral species (McMahon et al., 2018). We would therefore expect a direct correspondence of coral skeleton and sinking POM, if coral $\delta^{13}C_{EAA}$ values are accurately recording export production baseline $\delta^{13}C$ values. In this study, however, we observed slightly elevated $\delta^{13}C_{EAA}$ values in coral skeletons than in sinking particles (by 2.0 ± 1.3‰; Fig. 7a). While such $\delta^{13}C_{EAA}$ offset might seem incongruous, it is exactly consistent with expected onshore/ offshore $\delta^{13}C$ production gradients on California margin. As noted above (methods) our coral collection site was located more inshore (near the mouth of Monterey Bay), characterized by somewhat higher productivity and more positive $\delta^{13}C$ values of surface POM, in comparison to the somewhat less productive, more offshore sediment trap site (Chavez et al., 1991; Miller et al., 2008). Prior data from deep-sea bamboo corals collected along the central California margin have shown exactly this same trend, with bulk $\delta^{13}C$ values increasing from offshore sites to nearshore sites (Hill et al., 2014), consistent with the positive $\delta^{13}C$ offset between corals and sediment traps we observe. Overall, given the complex export patterns and spatially heterogeneous productivity of Monterey Bay (Chavez et al., 1991), we consider this degree of agreement in $\delta^{13}C_{EAA}$ values between the two sample sets to be quite close.

4.5. Can proteinaceous deep-sea coral CSI-AA reconstruct surface ocean conditions?

The ultimate goal of this study was to evaluate the robustness of CSI-AA applications in paleoarchival coral skeletons. As discussed above (Section 4.4.4), a geographic offset in $\delta^{13}C_{EAA}$ values was observed between the corals and sediment trap samples. Therefore, we reconstructed and evaluated only the nitrogen records.

The $\delta^{15}N_{export\ production}$, source nitrogen $\delta^{15}N$, and exported $TP_{CSI\text{-}AA}$ values reconstructed using the coral $\delta^{15}N_{AA}$ data compared well with the reference records, particularly after correcting for the minor trophic transfer fractionation (by 0.6‰) in Phe values (Fig. 8). It thus appears that the observed $\delta^{15}N_{Phe}$ offsets between coral skeletons and sediment traps, although small, are real and likely linked to the expected small trophic fractionation in Phe values. This inference may also extend to other coral genera, but constraining the potential range of this metabolic/trophic transfer effect requires direct examination in other coral species. Overall, these results support our main conclusion of faithful preservation of CSI-AA-based proxies in coral skeletons and also highlight the robust performance of empirical models for reconstructing bulk isotope values of export production in Monterey Bay.

Applicability of these empirical models to other oceanic regions remains to be tested. The specific values of our models might potentially be applicable in similar highly productive ocean margin systems. However, given the general regional disparities in environmental conditions, source of nutrients (e.g., N_2 vs. nitrate), and composition and physiological status of plankton communities, region-specific model parameterization using suitable sample sets is likely needed. Supporting this idea are the results from several previous CSI-AA studies, which used empirical models derived from laboratory phytoplankton cultures to estimate bulk $\delta^{13}C$ values of primary production from $\delta^{13}C_{EAA}$ values (e.g., Schiff et al., 2014; Vokhshoori et al. 2014). A direct application of these culture-derived models to our sediment trap $\delta^{13}C_{EAA}$ time series produced $\delta^{13}C_{export\ production}$ values that had the same temporal trends, but were 1–3‰ more positive than our field measurements (Fig. EA5). This suggests the laboratory culture organisms used previously did not well reflect the mix of actual organisms contributing to export production in Monterey Bay. We therefore suggest using sediment trap samples from the region of interest with paired bulk and amino acid isotope values for model retraining.

Our data also suggest that prior to the implementation of models in coral archives, it will be useful to determine the spatial patterns of primary and export production in the study region. This can greatly improve the accuracy of biogeochemical and ecological reconstructions. For example, we observed a +2‰ offset in $\delta^{13}C_{EAA}$ between the inshore coral and offshore sediment trap, which we have hypothesized is due to the combined effect of onshore/offshore gradient in primary production $\delta^{13}C$ and the horizontal export of primary production (Chavez et al., 1991; Olivieri and Chavez, 2000; Pennington et al., 2010). As a consequence, applying $\delta^{13}C_{EAA}$ to the inshore coral with-

out first correcting this offset could overestimate the $\delta^{13}C$ values of primary and export production for offshore region. Nevertheless, even for a system without such contextual data, the CSI-AA records should still be able to reveal the temporal fluctuations of isotope values of primary and export production and the associated overlying ocean conditions.

Further, the results from our contemporaneous corals suggest great promise for extending the CSI-AA-based proxies to older coral skeletons for paleoceanographic study. Amino acids preserved in the deep-sea proteinaceous coral skeletons are highly resistant to decomposition (Strzepek et al., 2014; McMahon et al., 2015) and could therefore retain their isotopic compositions that allow reconstructions of export production isotope values, source nitrogen isotope values, and plankton food web trophic structure from both living and fossil specimens. On the California margin specifically, we suggest that CSI-AA and our new empirical models can now be applied to older bamboo corals in this region to reconstruct high-resolution ecosystem changes over at least centennial time scales. There are also other deep-sea coral genera that have far greater longevity (e.g., corals *Gerardia* sp. and *Leiopathes* sp.; Roark et al., 2009), which bears the potential to unveil millennial or longer records when the calibrated models are in place.

5. SUMMARY & CONCLUSIONS

This study has presented the first coupled bulk and amino acid $\delta^{13}C$ and $\delta^{15}N$ values for a multi-year sediment trap time series, and then exploited these data by comparing to contemporaneous deep-sea proteinaceous corals, to address a series of fundamental questions concerning the CSI-AA paleo-applications. Our main goal was confirmation of the use of a range of CSI-AA parameters preserved in deep sea coral skeletons as direct proxies for upper ocean biogeochemical and ecological history. We found that the compound-specific baseline proxies $\delta^{13}C_{EAA}$ and $\delta^{15}N_{Phe}$ in sinking particles accurately reproduce bulk $\delta^{13}C$ and $\delta^{15}N$ values of export production over multi-year time scales. Importantly, variations in essential and source AA isotope values in sinking particles were independent of carbon flux, trophic transfer, biodegradation and microbial resynthesis, together indicating excellent preservation of CSI-AA baseline proxies during export from the surface to deep ocean, and ultimately either into corals or sedimentary burial. The temporal patterns observed in several CSI-AA-based proxies (e.g., $\delta^{15}N_{Phe}$, $TP_{CSI\text{-}AA}$) also reflected major biogeochemical and ecological changes in surface ocean, such as seasonal shifts in plankton structures and occurrence of unusual dynamical conditions (e.g., El Niño), reinforcing the potential of these proxies in archives to construct similar climate shifts.

Sinking particle CSI-AA values matched those in geographically close deep-sea corals extremely well, further reinforcing the fidelity with which these values reflect those in sinking particle. We did observe small (1–2‰) isotopic enrichments in essential AA $\delta^{13}C$ and source AA $\delta^{15}N$ values. However, these differences were in the range expected based on isotope and production variations in the Monterey Bay: the $\delta^{13}C_{EAA}$ offsets matched expected geographic gradients in $\delta^{13}C$ values of primary production within Monterey Bay region. For nitrogen, while the source AA $\delta^{15}N$ offsets (~1‰) were near limits of analytical variation, we suggest they reflect the expected small trophic fractionations for Phe and Lys. We therefore propose that applying a small correction for trophic fractionation of source AA $\delta^{15}N$ in coral paleoarchives can improve the accuracy of reconstructions.

In contrast, we observed substantial ^{15}N enrichments for both Gly and Ser strongly indicating these AA do not act as "source" AA in deep sea corals. Coupled with recent literature documenting similar behaviors in other taxa, we propose that Gly and Ser should be considered within a new "intermediate" AA classification, at least in corals or higher-level marine consumers. In addition, using recently published corrections between coral skeleton and polyp (McMahon et al., 2018), we were able to calculate the first TDF_{AA} values for deep-sea corals. The $TDF_{Glx\text{-}Phe}$ value for the animal (i.e. living polyp) was 7.9‰, almost identical to the commonly used 7.6‰ value, confirming that the standard $TP_{CSI\text{-}AA}$ equation (Eq. (2)) is accurate for deep sea coral proxy applications, and the calibration findings of McMahon et al. (2018). However, the TDF calculations also indicated extremely high, but repeatable, $\delta^{15}N$ TDF values for Val, Ile, and Leu in coral skeletal protein. While this result bears further investigation, it suggests that multi-AA approaches for estimating trophic position are likely not applicable to coral archives.

Finally, building on our new empirical models (e.g., Eq. (6)) and observed offsets in CSI-AA baseline values (e.g., $\delta^{15}N_{Phe}$), we directly demonstrate for the first time that CSI-AA in deep-sea coral skeletons are able to reconstruct contemporaneous $\delta^{15}N_{bulk}$ values of export production, source nitrogen $\delta^{15}N$ values, and exported $TP_{CSI\text{-}AA}$ values with good accuracy. These new results demonstrate that key CSI-AA-based proxies remain accurate, despite degradation and major flux attenuation, in deep-exported POM, transmitting a record of surface ocean processes into deep sea, and ultimately coral or sedimentary archives. Taken together, these new data have wide-ranging implications for CSI-AA biogeochemical and ecological applications, providing novel insight into the systematics of AA isotope values in export production, while representing the first direct field-based validation for emerging CSI-AA paleoceanographic studies (e.g., Sherwood et al., 2011; Sherwood et al., 2014; McMahon et al., 2015; Williams et al., 2017). We suggest that future work calibrating our empirical models for different oceanic regions will allow extension of these approaches to deep-sea protein coral archives worldwide.

Declaration of Competing Interest

The authors declare that they have no known competing financial interests or personal relationships that could have appeared to influence the work reported in this paper.

ACKNOWLEDGEMENTS

We would like to acknowledge the crew of the R/V *Point Sur* and R/V *Western Flyer* for assistance with sediment

trap and coral samplings. We thank Stephanie Christensen for assistance with CSI-AA analysis. This study was supported by National Science Foundation (OCE 1635527 to T.G. and M.M). A portion of this work was performed under the auspices of the U.S. Department of Energy (DE-AC52-07NA27344).

RESEARCH DATA

Research Data associated with this article can be accessed at https://doi.org/10.17632/6hy8tsrkf9.2 and will be submitted to BCO-DMO.

APPENDIX A. SUPPLEMENTARY MATERIAL

Supplementary data to this article can be found online at https://doi.org/10.1016/j.gca.2020.12.012.

REFERENCES

Altabet M. A., Deuser W. G., Honjo S. and Stienen C. (1991) Seasonal and depth-related changes in the source of sinking particles in the North Atlantic. *Nature* **354**, 136–139.

Altabet M. A., Pilskaln C., Thunell R., Pride C., Sigman D., Chavez F. and Francois R. (1999) The nitrogen isotope biogeochemistry of sinking particles from the margin of the Eastern North Pacific. *Deep-Sea Res. Pt. I* **46**, 655–679.

Batista F. C., Ravelo A. C., Crusius J., Casso M. A. and McCarthy M. D. (2014) Compound specific amino acid δ15N in marine sediments: A new approach for studies of the marine nitrogen cycle. *Geochim. Cosmochim. Acta* **142**, 553–569.

Beaulieu S. E. and Smith K. L. (1998) Phytodetritus entering the benthic boundary layer and aggregated on the sea floor in the abyssal NE Pacific: macro- and microscopic composition. *Deep-Sea Res. Part II Top. Stud. Oceanogr.* **45**, 781–815.

Berg, J., Tymoczko, J., Stryer, L., Stryer, L., 2002. Biochemistry. In: Freeman, W. (Ed.), 5th ed., New York, p. 992.

Calleja M. L., Batista F., Peacock M., Kudela R. and McCarthy M. D. (2013) Changes in compound specific δ15N amino acid signatures and d/l ratios in marine dissolved organic matter induced by heterotrophic bacterial reworking. *Mar. Chem.* **149**, 32–44.

Castro C. G., Chavez F. P., Pennington J. T., Durazo R. and Collins C. A. (2018) Temporal variability of downward fluxes of organic carbon off Monterey Bay. *Deep-Sea Res. Part II Top. Stud. Oceanogr.* **151**, 89–101.

Chavez F. P. (1996) Forcing and biological impact of onset of the 1992 El Niño in central California. *Geophys. Res. Lett.* **23**, 265–268.

Chavez F. P., Barber R. T., Kosro P. M., Huyer A., Ramp S. R., Stanton T. P. and Rojas de Mendiola B. (1991) Horizontal transport and the distribution of nutrients in the coastal transition zone off northern California: effects on primary production, phytoplankton biomass and species composition. *J. Geophys. Res.-Oceans* **96**, 14833–14848.

Chavez F. P., Pennington J. T., Michisaki R. P., Blum M., Chavez G. M., Friederich J., Jones B., Herlien R., Kieft B. and Hobson B. (2017) Climate variability and change: Response of a coastal ocean ecosystem. *Oceanography* **30**, 128–145.

Chikaraishi Y., Kashiyama Y., Ogawa N. O., Kitazato H. and Ohkouchi N. (2007) Metabolic control of nitrogen isotope composition of amino acids in macroalgae and gastropods: implications for aquatic food web studies. *Mar. Ecol. Prog. Ser.* **342**, 85–90.

Chikaraishi Y., Ogawa N. O., Kashiyama Y., Takano Y., Suga H., Tomitani A., Miyashita H., Kitazato H. and Ohkouchi N. (2009) Determination of aquatic food-web structure based on compound-specific nitrogen isotopic composition of amino acids. *Limnol. Oceanogr. Meth.* **7**, 740–750.

Dauwe B., Middelburg J., Herman P. and Heip C. (1999) Linking diagenetic alteration of amino acids and bulk organic matter reactivity. *Limnol. Oceanogr.* **44**, 1809–1814.

Décima M., Landry M. R. and Popp B. N. (2013) Environmental perturbation effects on baseline δ15N values and zooplankton trophic flexibility in the southern California Current Ecosystem. *Limnol. Oceanogr.* **58**, 624–634.

Dore J. E., Brum J. R., Tupas L. M. and Karl D. M. (2002) Seasonal and interannual variability in sources of nitrogen supporting export in the oligotrophic subtropical North Pacific Ocean. *Limnol. Oceanogr.* **47**, 1595–1607.

Ehrlich H. (2010) *Biological Materials of Marine Origin*. Springer.

Fawcett S. and Ward B. (2011) Phytoplankton succession and nitrogen utilization during the development of an upwelling bloom. *Mar. Ecol. Prog. Ser.* **428**, 13–31.

Fogel M. L. and Tuross N. (1999) Transformation of plant biochemicals to geological macromolecules during early diagenesis. *Oecologia* **120**, 336–346.

Fry B. and Sherr E. B. (1989) δ13C measurements as indicators of carbon flow in marine and freshwater ecosystems. In *Stable Isotopes in Ecological Research*. Springer, pp. 196–229.

Galbraith E. D., Kienast M., Albuquerque A. L., Altabet M. A., Batista F., Bianchi D., Calvert S. E., Contreras S., Crosta X. and De Pol-Holz R. (2013) The acceleration of oceanic denitrification during deglacial warming. *Nat. Geosci.* **6**, 579–584.

Germain L. R., Koch P. L., Harvey J. and McCarthy M. D. (2013) Nitrogen isotope fractionation in amino acids from harbor seals: implications for compound-specific trophic position calculations. *Mar. Ecol. Prog. Ser.* **482**, 265–277.

Glynn D. S., McMahon K. W., Guilderson T. P. and McCarthy M. D. (2019) Major shifts in nutrient and phytoplankton dynamics in the North Pacific Subtropical Gyre over the last 5000 years revealed by high-resolution proteinaceous deep-sea coral δ15N and δ13C records. *Earth Planet. Sci. Lett.* **515**, 145–153.

Goericke R. and Fry B. (1994) Variations of marine plankton δ13C with latitude, temperature, and dissolved CO2 in the world ocean. *Global Biogeochem. Cycl.* **8**, 85–90.

Guilderson T. P., McCarthy M., Dunbar R., Englebrecht A. and Roark E. (2013) Late Holocene variations in Pacific surface circulation and biogeochemistry inferred from proteinaceous deep-sea corals. *Biogeosciences* **10**, 6019–6028.

Hannides C., Popp B. N., Choy C. A. and Drazen J. C. (2013) Midwater zooplankton and suspended particle dynamics in the North Pacific Subtropical Gyre: A stable isotope perspective. *Limnol. Oceanogr.* **58**, 1931–1946.

Hannides C. C., Popp B. N., Landry M. R. and Graham B. S. (2009) Quantification of zooplankton trophic position in the North Pacific Subtropical Gyre using stable nitrogen isotopes. *Limnol. Oceanogr.* **54**, 50–61.

Hansman R. L., Griffin S., Watson J. T., Druffel E. R., Ingalls A. E., Pearson A. and Aluwihare L. I. (2009) The radiocarbon signature of microorganisms in the mesopelagic ocean. *Proc. Natl. Acad. Sci.* **106**, 6513–6518.

Hayes J. M., Strauss H. and Kaufman A. J. (1999) The abundance of 13C in marine organic matter and isotopic fractionation in the global biogeochemical cycle of carbon during the past 800 Ma. *Chem. Geol.* **161**, 103–125.

Hill T., Myrvold C., Spero H. and Guilderson T. (2014) Evidence for benthic–pelagic food web coupling and carbon export from

California margin bamboo coral archives. *Biogeosciences* **11**, 3845–3854.

Hoen D. K., Kim S. L., Hussey N. E., Wallsgrove N. J., Drazen J. C. and Popp B. N. (2014) Amino acid 15N trophic enrichment factors of four large carnivorous fishes. *J. Exp. Mar. Biol. Ecol.* **453**, 76–83.

Honjo S. and Doherty K. W. (1988) Large aperture time-series sediment traps; design objectives, construction and application. *Deep-Sea Res. Pt. I* **35**, 133–149.

Howland M. R., Corr L. T., Young S. M., Jones V., Jim S., Van Der Merwe N. J., Mitchell A. D. and Evershed R. P. (2003) Expression of the dietary isotope signal in the compound-specific δ13C values of pig bone lipids and amino acids. *Int. J. Osteoarchaeol.* **13**, 54–65.

Jim S., Jones V., Ambrose S. H. and Evershed R. P. (2006) Quantifying dietary macronutrient sources of carbon for bone collagen biosynthesis using natural abundance stable carbon isotope analysis. *Br. J. Nutr.* **95**, 1055–1062.

Kudela R. and Dugdale R. (2000) Nutrient regulation of phytoplankton productivity in Monterey Bay, California. *Deep-Sea Res. Part II Top. Stud. Oceanogr.* **47**, 1023–1053.

Larsen T., Taylor D. L., Leigh M. B. and O'Brien D. M. J. E. (2009) Stable isotope fingerprinting: a novel method for identifying plant, fungal, or bacterial origins of amino acids. *Ecology* **90**, 3526–3535.

McCarthy M. D., Benner R., Lee C. and Fogel M. L. (2007) Amino acid nitrogen isotopic fractionation patterns as indicators of heterotrophy in plankton, particulate, and dissolved organic matter. *Geochim. Cosmochim. Acta* **71**, 4727–4744.

McCarthy M. D., Lehman J. and Kudela R. (2013) Compound-specific amino acid δ15N patterns in marine algae: Tracer potential for cyanobacterial vs. eukaryotic organic nitrogen sources in the ocean. *Geochim. Cosmochim. Acta* **103**, 104–120.

McClelland J. W. and Montoya J. P. (2002) Trophic relationships and the nitrogen isotopic composition of amino acids in plankton. *Ecology* **83**, 2173–2180.

McMahon K. W., Fogel M. L., Elsdon T. S. and Thorrold S. R. (2010) Carbon isotope fractionation of amino acids in fish muscle reflects biosynthesis and isotopic routing from dietary protein. *J. Anim. Ecol.* **79**, 1132–1141.

McMahon K. W. and McCarthy M. D. (2016) Embracing variability in amino acid δ15N fractionation: mechanisms, implications, and applications for trophic ecology. *Ecosphere* **7**, 1–26.

McMahon K. W., McCarthy M. D., Sherwood O. A., Larsen T. and Guilderson T. P. (2015) Millennial-scale plankton regime shifts in the subtropical North Pacific Ocean. *Science* **350**, 1530–1533.

McMahon K. W., Williams B., Guilderson T. P., Glynn D. S. and McCarthy M. D. (2018) Calibrating amino acid δ13C and δ15N offsets between polyp and protein skeleton to develop proteinaceous deep-sea corals as paleoceanographic archives. *Geochim. Cosmochim. Acta* **220**, 261–275.

Messié M. and Chavez F. P. (2017) Nutrient supply, surface currents, and plankton dynamics predict zooplankton hotspots in coastal upwelling systems. *Geophys. Res. Lett.* **44**, 8979–8986.

Miller T. W., Brodeur R. D. and Rau G. H. (2008) Carbon stable isotopes reveal relative contribution of shelf-slope production to the Northern California Current pelagic community. *Limnol. Oceanogr.* **53**, 1493–1503.

Montes E., Thunell R., Muller-Karger F. E., Lorenzoni L., Tappa E., Troccoli L., Astor Y. and Varela R. (2013) Sources of δ15N variability in sinking particulate nitrogen in the Cariaco Basin, Venezuela. *Deep-Sea Res. Part II Top. Stud. Oceanogr.* **93**, 96–107.

Nakatsuka T., Handa N., Wada E. and Wong C. S. (1992) The dynamic changes of stable isotopic ratios of carbon and nitrogen in suspended and sedimented particulate organic matter during a phytoplankton bloom. *J. Mar. Res.* **50**, 267–296.

Nielsen J. M., Popp B. N. and Winder M. (2015) Meta-analysis of amino acid stable nitrogen isotope ratios for estimating trophic position in marine organisms. *Oecologia* **178**, 631–642.

O'Connell T. C. (2017) 'Trophic'and 'source'amino acids in trophic estimation: a likely metabolic explanation. *Oecologia* **184**, 317–326.

Ohkouchi N., Chikaraishi Y., Close H. G., Fry B., Larsen T., Madigan D. J., McCarthy M. D., McMahon K. W., Nagata T. and Naito Y. I. (2017) Advances in the application of amino acid nitrogen isotopic analysis in ecological and biogeochemical studies. *Org. Geochem.* **113**, 150–174.

Olivieri R. A. and Chavez F. P. (2000) A model of plankton dynamics for the coastal upwelling system of Monterey Bay, California. *Deep-Sea Res. Part II Top. Stud. Oceanogr.* **47**, 1077–1106.

Pennington J. T. and Chavez F. P. (2000) Seasonal fluctuations of temperature, salinity, nitrate, chlorophyll and primary production at station H3/M1 over 1989–1996 in Monterey Bay, California. *Deep-Sea Res. Part II Top. Stud. Oceanogr.* **47**, 947–973.

Pennington J. T., Friederich G. E., Castro C. G., Collins C. A., Evans W. W. and Chavez F. P. (2010) The Northern and Central California Coastal Upwelling System: A Global Synthesis. In *Carbon and Nutrient Fluxes in Continental Margins* (eds. K.-K. Liu, L. Atkinson, R. Quinones and L. Talaue-McManus). Springer, Heidelberg, pp. 29–44.

Peterson B. J. and Fry B. (1987) Stable isotopes in ecosystem studies. *Annu. Rev. Ecol. Syst.* **18**, 293–320.

Pilskaln C. H., Lehmann C., Paduan J. B. and Silver M. W. (1998) Spatial and temporal dynamics in marine aggregate abundance, sinking rate and flux: Monterey Bay, central California. *Deep-Sea Res. Part II Top. Stud. Oceanogr.* **45**, 1803–1837.

Pilskaln C. H., Paduan J. B., Chavez F. P., Anderson R. Y. and Berelson W. M. (1996) Carbon export and regeneration in the coastal upwelling system of Monterey Bay, central California. *J. Mar. Res.* **54**, 1149–1178.

Popp B. N., Graham B. S., Olson R. J., Hannides C. C., Lott M. J., López-Ibarra G. A., Galván-Magaña F. and Fry B. (2007) Insight into the trophic ecology of yellowfin tuna, Thunnus albacares, from compound-specific nitrogen isotope analysis of proteinaceous amino acids. *Terrestr. Ecol.* **1**, 173–190.

Post D. M. (2002) Using stable isotopes to estimate trophic position: models, methods, and assumptions. *Ecology* **83**, 703–718.

Prouty N., Roark E., Buster N. and Ross S. W. (2011) Growth rate and age distribution of deep-sea black corals in the Gulf of Mexico. *Mar. Ecol. Prog. Ser.* **423**, 101–115.

Prouty N. G., Roark E. B., Koenig A. E., Demopoulos A. W., Batista F. C., Kocar B. D., Selby D., McCarthy M. D., Mienis F. and Ross S. W. (2014) Deep-sea coral record of human impact on watershed quality in the Mississippi River Basin. *Global Biogeochem. Cycl.* **28**, 29–43.

Rau G. H., Low C., Pennington J. T., Buck K. R. and Chavez F. P. (1998) Suspended particulate nitrogen δ15N versus nitrate utilization: observations in Monterey Bay, CA. *Deep-Sea Res. Part II Top. Stud. Oceanogr.* **45**, 1603–1616.

Rau G. H., Chavez F. P. and Friederich G. E. (2001) Plankton 13C/12C variations in Monterey Bay, California: evidence of non-diffusive inorganic carbon uptake by phytoplankton in an upwelling environment. *Deep-Sea Res. Pt. I* **48**, 79–94.

Rau G. H., Ohman M. D. and Pierrot-Bults A. (2003) Linking nitrogen dynamics to climate variability off central California: a 51 year record based on 15N/14N in CalCOFI zooplankton. *Deep-Sea Res. Part II Top. Stud. Oceanogr.* **50**, 2431–2447.

Roark E. B., Guilderson T. P., Dunbar R. B., Fallon S. J. and Mucciarone D. A. (2009) Extreme longevity in proteinaceous deep-sea corals. *Proc. Natl. Acad. Sci.* **106**, 5204–5208.

Roark E. B., Guilderson T. P., Flood-Page S., Dunbar R. B., Ingram B. L., Fallon S. J. and McCulloch M. (2005) Radiocarbon-based ages and growth rates of bamboo corals from the Gulf of Alaska. *Geophys. Res. Lett.* **32**, L04606.

Rosenfeld L. K., Schwing F. B., Garfield N. and Tracy D. E. (1994) Bifurcated flow from an upwelling center: a cold water source for Monterey Bay. *Cont. Shelf Res.* **14**, 931–964.

Ruiz-Cooley R. I., Koch P. L., Fiedler P. C. and McCarthy M. D. (2014) Carbon and nitrogen isotopes from top predator amino acids reveal rapidly shifting ocean biochemistry in the outer California Current. *PloS one* **9**, e110355.

Sabadel A., Van Oostende N., Ward B., Woodward E., Van Hale R. and Frew R. (2019) Characterization of particulate organic matter cycling during a summer North Atlantic phytoplankton bloom using amino acid C and N stable isotopes. *Mar. Chem.* **214**, 103670.

Schiff J. T., Batista F. C., Sherwood O. A., Guilderson T. P., Hill T. M., Ravelo A. C., McMahon K. W. and McCarthy M. D. (2014) Compound specific amino acid δ13C patterns in a deep-sea proteinaceous coral: implications for reconstructing detailed δ13C records of exported primary production. *Mar. Chem.* **166**, 82–91.

Shanks A. L. and Trent J. D. (1980) Marine snow: sinking rates and potential role in vertical flux. *Deep-Sea Res. Pt. I* **27**, 137–143.

Sherwood O. A. and Edinger E. N. (2009) Ages and growth rates of some deep-sea gorgonian and antipatharian corals of Newfoundland and Labrador. *Can. J. Zool.* **66**, 142–152.

Sherwood O. A., Guilderson T. P., Batista F. C., Schiff J. T. and McCarthy M. D. (2014) Increasing subtropical North Pacific Ocean nitrogen fixation since the Little Ice Age. *Nature* **505**, 78–81.

Sherwood O. A., Heikoop J. M., Scott D. B., Risk M. J., Guilderson T. P. and McKinney R. A. (2005) Stable isotopic composition of deep-sea gorgonian corals Primnoa spp.: a new archive of surface processes. *Mar. Ecol. Prog. Ser.* **301**, 135–148.

Sherwood O. A., Lehmann M. F., Schubert C. J., Scott D. B. and McCarthy M. D. (2011) Nutrient regime shift in the western North Atlantic indicated by compound-specific δ15N of deep-sea gorgonian corals. *Proc. Natl. Acad. Sci.* **108**, 1011–1015.

Sherwood O. A., Scott D. B. and Risk M. J. (2006) Late Holocene radiocarbon and aspartic acid racemization dating of deep-sea octocorals. *Geochim. Cosmochim. Acta* **70**, 2806–2814.

Sherwood O. A., Thresher R. E., Fallon S. J., Davies D. M. and Trull T. W. (2009) Multi-century time-series of 15N and 14C in bamboo corals from deep Tasmanian seamounts: evidence for stable oceanographic conditions. *Mar. Ecol. Prog. Ser.* **397**, 209–218.

Silfer J., Engel M., Macko S. and Jumeau E. (1991) Stable carbon isotope analysis of amino acid enantiomers by conventional isotope ratio mass spectrometry and combined gas chromatography/isotope ratio mass spectrometry. *Anal. Chem.* **63**, 370–374.

Smith D. C., Simon M., Alldredge A. L. and Azam F. (1992) Intense hydrolytic enzyme-activity on marine aggregates and implications for rapid particle dissolution. *Nature* **359**, 139–142.

Steffan S. A., Chikaraishi Y., Currie C. R., Horn H., Gaines-Day H. R., Pauli J. N., Zalapa J. E. and Ohkouchi N. (2015) Microbes are trophic analogs of animals. *Proc. Natl. Acad. Sci.* **112**, 15119–15124.

Strzepek K., Thresher R., Revill A., Smith C., Komugabe A. and Fallon S. (2014) Preservation effects on the isotopic and elemental composition of skeletal structures in the deep-sea bamboo coral Lepidisis spp. (Isididae). *Deep-Sea Res Part II Top. Stud. Oceanogr.* **99**, 199–206.

Thresher R., Rintoul S. R., Koslow J. A., Weidman C., Adkins J. and Proctor C. (2004) Oceanic evidence of climate change in southern Australia over the last three centuries. *Geophys. Res. Lett.* **31**, L07212.

Thunell R. C. and Kepple A. B. (2004) Glacial-Holocene δ15N record from the Gulf of Tehuantepec, Mexico: Implications for denitrification in the eastern equatorial Pacific and changes in atmospheric N2O. *Global Biogeochem. Cycl.* **18**, GB1001.

Vokhshoori N. L., Larsen T. and McCarthy M. D. (2014) Reconstructing δ13C isoscapes of phytoplankton production in a coastal upwelling system with amino acid isotope values of littoral mussels. *Mar. Ecol. Prog. Ser.* **504**, 59–72.

Wankel S. D., Kendall C., Pennington J. T., Chavez F. P. and Paytan A. (2007) Nitrification in the euphotic zone as evidenced by nitrate dual isotopic composition: Observations from Monterey Bay, California. *Global Biogeochem. Cycles* **21**, GB2009.

Wilkerson F., Dugdale R., Kudela R. and Chavez F. (2000) Biomass and productivity in Monterey Bay, California: contribution of the large phytoplankton. *Deep-Sea Res. Part II Top. Stud. Oceanogr.* **47**, 1003–1022.

Williams B., Thibodeau B., Chikaraishi Y., Ohkouchi N., Walnum A., Grottoli A. G. and Colin P. L. (2017) Consistency in coral skeletal amino acid composition offshore of Palau in the western Pacific warm pool indicates no impact of decadal variability in nitricline depth on primary productivity. *Limnol. Oceanogr.* **62**, 399–407.

Woodworth M., Goñi M., Tappa E., Tedesco K., Thunell R., Astor Y., Varela R., Diaz-Ramos J. R. and Müller-Karger F. (2004) Oceanographic controls on the carbon isotopic compositions of sinking particles from the Cariaco Basin. *Deep-Sea Res. Pt. I* **51**, 1955–1974.

Yamaguchi Y. T., Chikaraishi Y., Takano Y., Ogawa N. O., Imachi H., Yokoyama Y. and Ohkouchi N. (2017) Fractionation of nitrogen isotopes during amino acid metabolism in heterotrophic and chemolithoautotrophic microbes across Eukarya, Bacteria, and Archaea: Effects of nitrogen sources and metabolic pathways. *Org. Geochem.* **111**, 101–112.

Associate editor: Thomas Wagner

Electronic Annex

Amino acid $\delta^{13}C$ and $\delta^{15}N$ patterns from sediment trap time series and deep-sea corals: implications for biogeochemical and ecological reconstructions in paleoarchives

Yuan Shen [a,b*], Thomas P. Guilderson [b,c], Owen A. Sherwood [b,d], Carmen G. Castro [e], Francisco P. Chavez [f], Matthew D. McCarthy [b]

[a] *State Key Laboratory of Marine Environmental Science & College of Ocean and Earth Sciences, Xiamen University, Xiamen, Fujian 361102, P. R. China*

[b] *Ocean Sciences Department, University of California, Santa Cruz, 1156 High Street, Santa Cruz, CA 95064, USA*

[c] *Lawrence Livermore National Laboratory, Livermore, CA 94550, USA*

[d] *Department of Earth Sciences, Dalhousie University, Halifax, Nova Scotia, B3H 4R2, Canada*

[e] *CSIC, Instituto de Investigaciones Marinas (IIM), Eduardo Cabello 6, 36208, Vigo, Spain*

[f] *Monterey Bay Aquarium Research Institute, Moss Landing, CA 95039, USA*

*Corresponding Author: Yuan Shen (yuanshen@xmu.edu.cn)

Table EA1. $\delta^{13}C$ and $\delta^{15}N$ values (‰) of individual amino acids in in-house reference standard (homogenized cyanobacteria) analyzed during each batch of field samples.

$\delta^{13}C$	Batch 1	Batch 2	Batch 3	Batch 4	Batch 5	Batch 6	Batch 7	Batch 8	Mean ± std
Ala	-17.1±0.2	-16.1±0.8	-15.6±0.4	-15.8±0.2	-14.9±0.0	-15.8±0.2	-16.4±0.8	-21.8±0.3	-16.7±2.2
Gly	-15.9±0.3	-17.9±0.1	-12.0±0.3	-13.6±0.6	-14.9±0.6	-17.2±0.1	-14.8±0.4	-17.5±0.1	-15.5±2.0
Thr	-19.7±0.9	-18.8±0.6	-15.5±0.2	-18.5±0.5	-16.3±0.6	-23.0±0.1	-11.9±0.4	-19.9±0.1	-18.0±3.4
Ser	-10.9±0.8	-12.2±0.1	-5.7±0.5	-8.4±0.3	-12.2±0.2	-12.0±0.4	-12.6±1.9	-12.6±0.1	-10.8±2.5
Val	-23.5±0.3	-26.5±0.4	-24.4±0.3	-23.3±0.4	-27.4±0.4	-22.5±0.4	-29.6±0.9	-22.4±0.4	-25.0±2.6
Leu	-28.4±0.4	-28.3±0.1	-28.1±0.3	-29.1±0.2	-30.2±0.3	-30.9±0.1	-31.3±0.2	-32.8±0.3	-29.9±1.7
Ile	-25.4±0.3	-25.6±0.3	-24.6±0.2	-24.9±0.2	-25.9±0.2	-27.1±0.2	-27.0±0.3	-25.1±0.5	-25.7±0.9
Nle	-29.1±0.2	-29.1±0.1	-28.3±0.1	-28.9±0.2	-29.5±0.5	-29.6±0.2	-29.7±0.5	-29.6±0.2	-29.2±0.5
Pro	-19.6±0.2	-20.4±0.8	-16.5±0.3	-18.2±0.3	-18.3±0.1	-19.4±0.1	-20.9±0.1	-20.6±0.2	-19.2±1.5
Asp	-15.3±0.2	-14.5±0.3	-13.1±0.1	-15.7±0.3	-15.4±0.1	-16.2±0.2	-17.8±0.3	-17.9±0.4	-15.7±1.6
Glu	-21.7±0.2	-20.0±0.3	-16.2±0.3	-19.2±0.3	-18.5±0.2	-18.8±0.0	-19.9±0.2	-20.6±0.3	-19.3±1.6
Phe	-26.6±0.3	-28.4±0.2	-26.1±0.2	-26.8±0.2	-28.4±0.2	-28.7±0.3	-29.1±0.7	-29.4±0.1	-27.9±1.2
Tyr	-22.7±1.0	-24.7±0.1	-17.7±0.5	-20.4±0.4	-22.3±0.4	-21.4±1.0	-22.8±0.4	-18.4±0.3	-21.3±2.3
Lys	-20.4±0.2	-20.3±0.1	-18.5±0.1	-20.1±0.2	-20.7±0.3	-20.9±0.3	-20.8±0.2	-22.0±0.2	-20.5±1.0

$\delta^{15}N$	Batch 1	Batch 2	Batch 3	Batch 4	Batch 5	Batch 6	Mean ± std
Ala	14.3±0.4	15.0±0.1	14.3±0.2	14.0±0.2	14.4±0.2	13.9±0.5	14.3±0.4
Gly	9.1±0.4	9.7±0.1	8.7±0.3	9.2±0.1	8.1±0.2	7.8±0.4	8.8±0.7
Thr	7.9±0.3	7.4±0.2	8.5±0.3	8.1±0.3	10.3±0.3	9.4±0.2	8.6±1.1
Ser	4.4±0.2	5.1±0.4	3.8±0.3	6.1±0.1	2.2±0.5	1.3±0.4	3.8±1.8
Val	10.0±0.2	9.3±0.3	9.6±0.1	9.4±0.2	12.0±0.5	11.7±0.5	10.3±1.2
Leu	6.6±0.6	9.0±0.1	7.8±0.5	7.5±0.5	6.0±0.2	6.4±0.1	7.2±1.1
Ile	7.1±0.7	4.9±0.2	7.8±1.2	8.5±0.6	6.5±0.4	7.1±0.3	7.0±1.2
Nle	8.6±0.0	9.4±0.2	9.1±0.3	9.1±0.3	8.2±0.4	8.7±0.2	8.9±0.4
Pro	10.5±0.1	10.7±0.1	10.6±0.5	10.0±0.7	10.5±0.9	10.7±0.2	10.5±0.3
Asp	8.0±0.2	8.3±0.2	8.5±0.4	8.5±0.2	8.2±0.6	8.7±0.1	8.4±0.3
Glu	7.5±0.1	8.8±0.1	7.9±0.4	8.4±0.1	6.3±0.1	6.0±0.2	7.5±1.1
Phe	7.3±0.6	8.4±0.4	6.8±0.9	7.6±0.2	6.2±0.2	6.9±0.5	7.2±0.7
Tyr	nd	nd	nd	nd	nd	nd	nd
Lys	6.0±0.4	7.6±0.9	5.6±0.7	4.5±0.6	6.5±0.5	5.5±0.7	6.0±1.1

One cyanobacteria standard was analyzed during each batch of sample measurement. Data for each batch are reported as average ± standard deviation of 3 injections. "Mean ± std" refers to the average and standard deviation value of the entire standard set (n = 8 for C; *n* = 6 for N). nd: not determined.

Table EA2. List of abbreviations and terminology used in this study.

Abbreviation/Terminology	Description
AA or AAs	Amino acids
Ala	Alanine
Asx	Asparagine + aspartic Acid
AVG	Average
Baseline isotope values	Refer to the source nitrogen $\delta^{15}N$ value or primary production $\delta^{13}C$ value
CSI-AA	Compound-specific isotope analysis of amino acids
CSI-AA-based proxies	Refer to $\delta^{13}C_{Phe}$, $\delta^{13}C_{EAA}$, $\delta^{15}N_{Phe}$, $\delta^{15}N_{SrcAA}$, or/and TP_{CSI-AA}
CSI-AA baseline proxies	Refer to $\delta^{13}C_{Phe}$, $\delta^{13}C_{EAA}$, $\delta^{15}N_{Phe}$ or/and $\delta^{15}N_{SrcAA}$
CSI-AA values	Refer to C and N isotope values of amino acids in general
DI	Degradation index (based on mol% values of protein AAs)
DIC	Dissolved Inorganic Carbon
EAA	Essential amino acids (Thr, Ile, Val, Phe, Leu, Lys)
Exported TP	Trophic position of export production
GC-IRMS	Gas chromatography isotope ratio mass spectrometry
Glx	Glutamine + Glutamic acid
Gly	Glycine
HCl	Hydrochloric acid
H_2SO_3	Sulfurous acid
Ile	Isoleucine
Leu	Leucine
Lys	Lysine
NEAA	Non-essential amino acids (Gly, Ser, Asx, Glx, Pro, Ala)
Phe	Phenylalanine
POC	Particulate organic carbon
POM	Particulate organic matter
Pro	Proline
Ser	Serine
Source nitrogen	Inorganic nitrogen used by primary producer (e.g., N_2 or nitrate)
SrcAA	Source amino acids (Phe, Lys)
ΣV	Sum of variance (based on $\delta^{15}N$ values of trophic amino acids)
STD	Standard deviation
TDF	Trophic discrimination factor
Thr	Threonine
TP	Trophic position
TP_{CSI-AA}	Trophic position estimated from $\delta^{15}N$ values of Glu and Phe
$TP_{skeleton}$	TP_{CSI-AA} values of coral skeletons
TrAA	Trophic amino acids (Glx, Asx, Ala, Leu, Ile, Pro, Val)
Val	Valine
VPDB	Vienna PeeDee Belemnite
$\delta^{13}C_{EAA}$	Mean $\delta^{13}C$ value of the six essential amino acids
$\delta^{13}C_{NEAA}$	Mean $\delta^{13}C$ value of the six non-essential amino acids
$\delta^{15}N_{SrcAA}$	Mean $\delta^{15}N$ value of the two source amino acids
$\delta^{15}N_{TrAA}$	Mean $\delta^{15}N$ value of the seven trophic amino acids
$\delta^{13}C_{export\ production}$	Bulk $\delta^{13}C$ value of sediment trap material (i.e., sinking particles)
$\delta^{15}N_{export\ production}$	Bulk $\delta^{15}N$ value of sediment trap material (i.e., sinking particles)

Table EA3. Estimated vs. measured $\delta^{13}C$ and $\delta^{15}N$ values (‰) of export production in Monterey Bay.

Samples	Collection date		$\delta^{13}C_{export\ production}$			$\delta^{15}N_{export\ production}$		
	Initial	Final	Measured	Estimated from sinking particle $\delta^{13}C_{Phe}$	Estimated from sinking particle δ^{13}_{EAA}	Measured	Reconstructed from sinking particle $\delta^{15}N_{Phe}$	Reconstructed from sinking particle$\delta^{15}N_{SrcAA}$
S2_2-10	12/30/98	1/13/99	-21.9	-21.2±0.1	-21.0±0.3	6.8	6.7±0.4	6.8±0.7
S2_4-3	9/1/99	9/15/99	nd	nd	nd	7.2	nd	nd
S2_4-12	1/5/00	1/19/00	-21.7	-21.1±0.4	-21.5±0.8	7.5	7.7±0.2	7.7±0.4
S2_5-5	4/5/00	4/19/00	nd	nd	nd	6.9	nd	nd
S2_7-13	1/31/01	2/14/01	-22.1	-22.6±0.1	-22.2±0.7	7.0	7.6±0.2	7.7±0.4
S2_7-12	2/14/01	2/28/01	-21.8	-22.4±0.1	-21.9±0.4	7.2	7.5±0.5	7.4±0.6
S2_7-11	2/28/01	3/14/01	-22.0	-22.1±0.2	-21.9±0.5	6.9	7.9±0.2	7.5±0.7
S2_7-10	3/14/01	3/28/01	-22.4	-21.6±0.5	-21.6±0.9	6.9	7.1±0.5	7.2±0.6
S2_9-1	2/8/02	2/20/02	-21.4	-21.7±0.2	-22.3±0.8	7.1	7.2±0.4	7.5±0.5
S2_9-6	4/17/02	5/1/02	-20.1	-21.4±0.1	-21.5±0.5	7.1	6.7±0.5	6.9±0.9
S2_9-13	7/24/02	8/7/02	-21.6	-21.7±0.2	-22.0±0.6	7.0	7.4±0.6	7.7±0.7
S2_10-6	11/13/02	11/27/02	-24.0	-23.9±0.2	-23.2±0.8	8.1	8.5±0.6	8.0±0.9
S2_10-7	11/27/02	12/11/02	-23.4	-22.6±0.7	-23.5±1.7	10.0	9.4±0.3	9.3±0.5
S2_10-8	12/11/02	12/25/02	-23.1	-22.4±0.2	-22.9±0.8	8.7	9.2±0.2	9.1±0.4
S2_10-9	12/25/02	1/8/03	-22.8	-22.4±0.4	-22.0±0.7	9.4	8.8±0.4	8.9±0.6
S2_10-10	1/8/03	1/22/03	-22.4	-21.7±0.3	-21.5±0.9	8.8	9.0±0.5	8.8±0.7
S2_10-11	1/22/03	2/5/03	-22.6	-22.9±0.1	-23.2±0.4	8.4	8.5±0.3	8.7±0.6
S2_10-12	2/5/03	2/19/03	-22.2	-21.6±0.7	-22.1±1.1	8.1	8.9±0.2	8.6±0.6
S2_10-13	2/19/03	3/5/03	-22.0	-22.6±0.2	-22.2±0.7	9.8	8.6±0.1	8.4±0.6
S2_12-1	9/10/03	9/24/03	-21.4	-21.7±0.3	-21.4±0.6	8.2	7.7±0.2	8.2±0.3
S2_12-7	12/3/03	12/17/03	-22.1	-21.0±0.2	-21.5±0.7	7.9	7.3±0.2	6.6±0.6
S2_13-4	4/28/04	5/12/04	-19.2	-20.6±0.3	-20.1±0.4	8.2	7.9±0.5	7.5±0.7
S2_13-9	7/7/04	7/21/04	-20.7	-21.7±0.2	-21.8±0.6	7.2	7.2±0.6	7.4±0.7
S2_14-3	11/8/04	12/6/04	-20.8	-20.9±0.1	-20.6±0.4	8.5	8.1±0.3	8.6±0.5
Flux-weighted Avg			*-21.5*	*-21.8*	*-21.7*	*7.8*	*7.8*	*7.8*
Flux-weighted Std			*1.3*	*0.9*	*0.9*	*0.9*	*0.8*	*0.7*

The estimated $\delta^{13}C_{export\ production}$ and $\delta^{15}N_{export\ production}$ were calculated from sediment trap (i.e., sinking particle) $\delta^{13}C_{EAA}$ and $\delta^{15}N_{phe}$ values using Eqs. (5) and (6), respectively. For comparison, the $\delta^{13}C_{export\ production}$ and $\delta^{15}N_{export\ production}$ values were re-estimated from sinking particle $\delta^{13}C_{Phe}$ and $\delta^{15}N_{SrcAA}$, respectively (see Figs. 3a, 3d for equations). The measured $\delta^{13}C_{export\ production}$ and $\delta^{15}N_{export\ production}$ values were the same as the $\delta^{13}C_{bulk}$ and $\delta^{15}N_{bulk}$ values in sinking particles. nd: not determined. These data were presented in Figs. 4 and EA1.

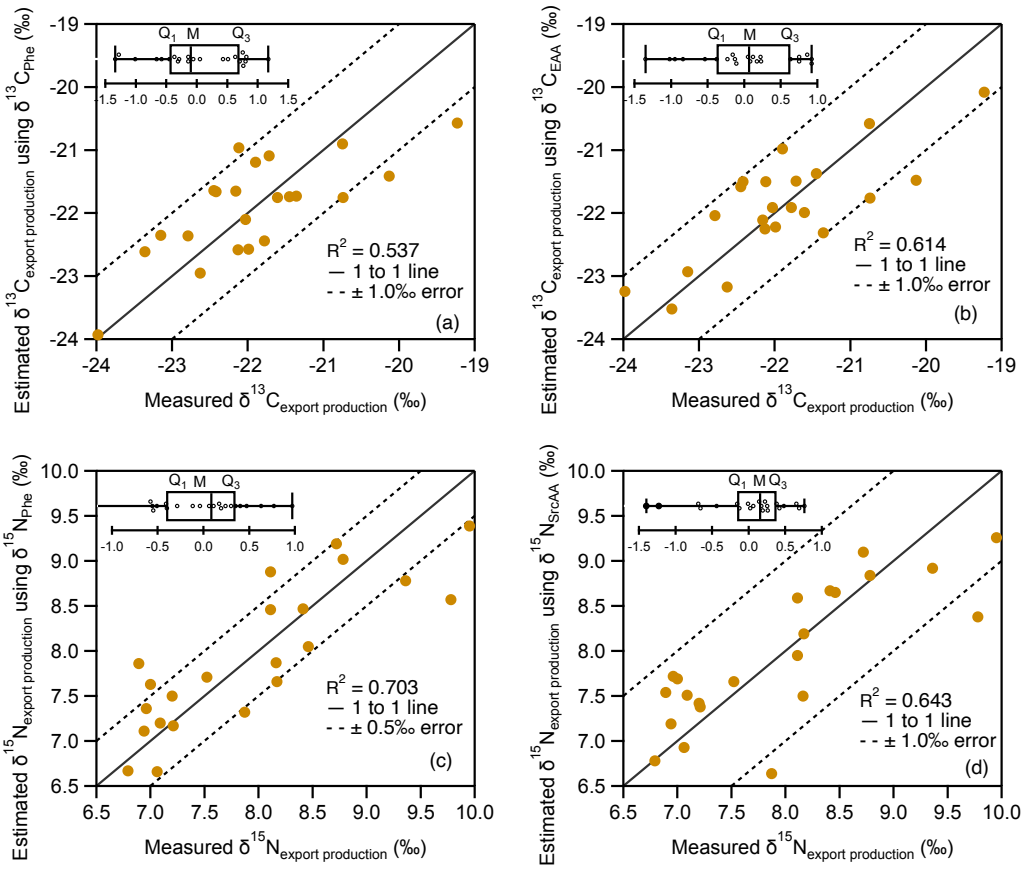

Figure EA1. Relationship between measured versus estimated bulk isotope values of export production and distribution of their offsets (inset plots). The results show that the bulk C and N isotope values of export production are best predicted from $\delta^{13}C_{EAA}$ (panel b) and $\delta^{15}N_{Phe}$ values (panel c), respectively. $\delta^{13}C_{export\ production}$ and $\delta^{15}N_{export\ production}$ values refer to the measured $\delta^{13}C_{bulk}$ and $\delta^{15}N_{bulk}$ values of sinking particles. The estimated $\delta^{13}C_{export\ production}$ values were calculated from sinking particle $\delta^{13}C_{Phe}$ (panel a) or $\delta^{13}C_{EAA}$ (panel b) values using equations shown in Figs. 3a and 3b. The estimated $\delta^{15}N_{export\ production}$ values were calculated from sinking particle $\delta^{15}N_{phe}$ (panel c) or $\delta^{15}N_{SrcAA}$ (panel d) values using equations shown in Figs. 3c and 3d. The solid black 1 to 1 lines show the theoretical predictions (i.e., with 100% accuracy), and the dashed lines bracket the range of predicted results with an error of ±1.0‰ or ±0.5‰. The inset boxplot represents the distribution of their offsets (i.e., estimation errors) (‰). Q1: first quartile, Q3: third quartile, M: median. In comparison, $\delta^{13}C_{export\ production}$ and $\delta^{15}N_{export\ production}$ values estimated using $\delta^{13}C_{Phe}$ and $\delta^{15}N_{SrcAA}$ showed larger errors compared to those from the $\delta^{13}C_{Phe}$ and $\delta^{15}N_{SrcAA}$ proxies (panels a and d).

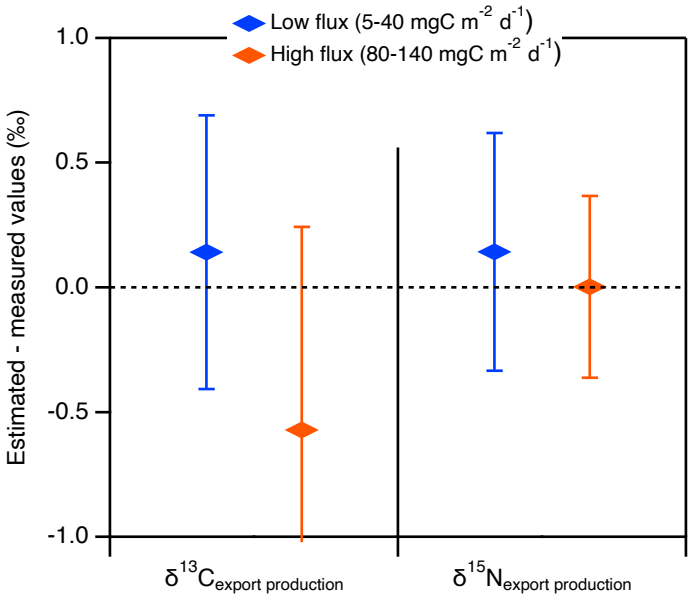

Figure EA2. Differences between the estimated and measured $\delta^{13}C$ and $\delta^{15}N$ values of export production during low and high carbon flux extremes. Error bars represent propagated standard deviations. The offsets between the estimated and measured records (i.e., errors of estimates) were relatively small (≤ 1.0‰) and were not significantly different between high and low carbon flux periods (Mann-Whitney *U*-Test, $p > 0.1$).

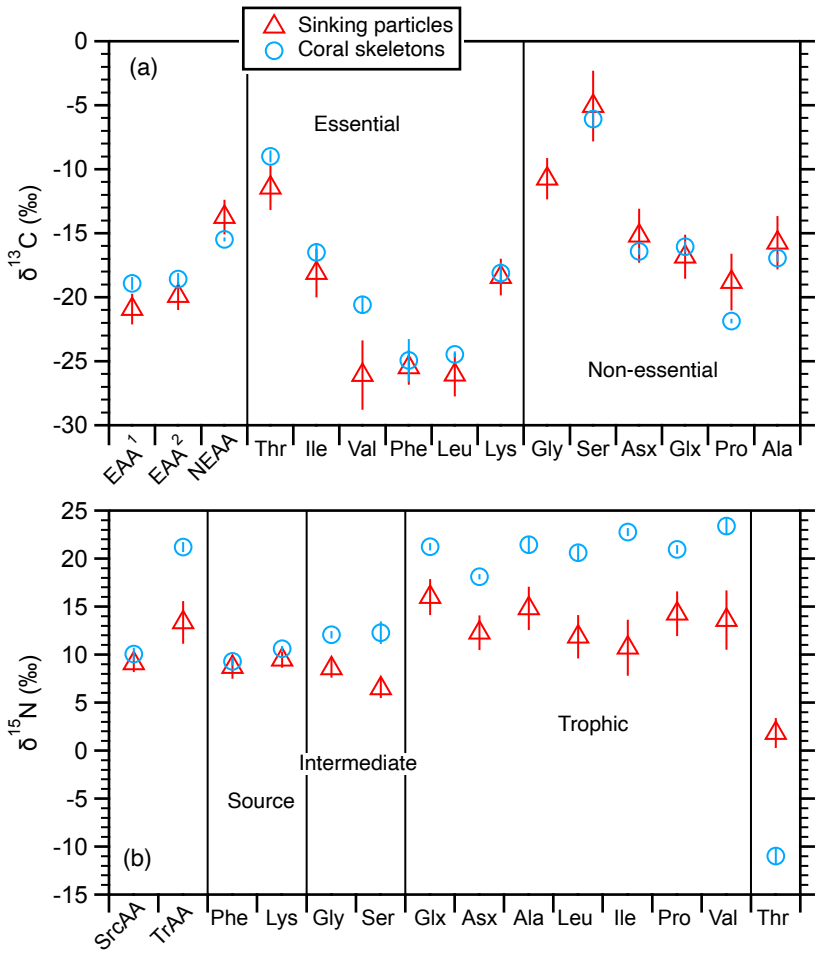

Figure EA3. Comparisons in mean amino acid $\delta^{13}C$ and $\delta^{15}N$ values between sinking particles and coral skeletons. Note that only the second and third skeletal peels were used to match the collection time of sinking particles. Error bar represents one standard deviation. EAA^1: average $\delta^{13}C$ value of all six essential AAs; EAA^2: average $\delta^{13}C$ value of essential AAs without Val. Gly was not determined in the coral samples.

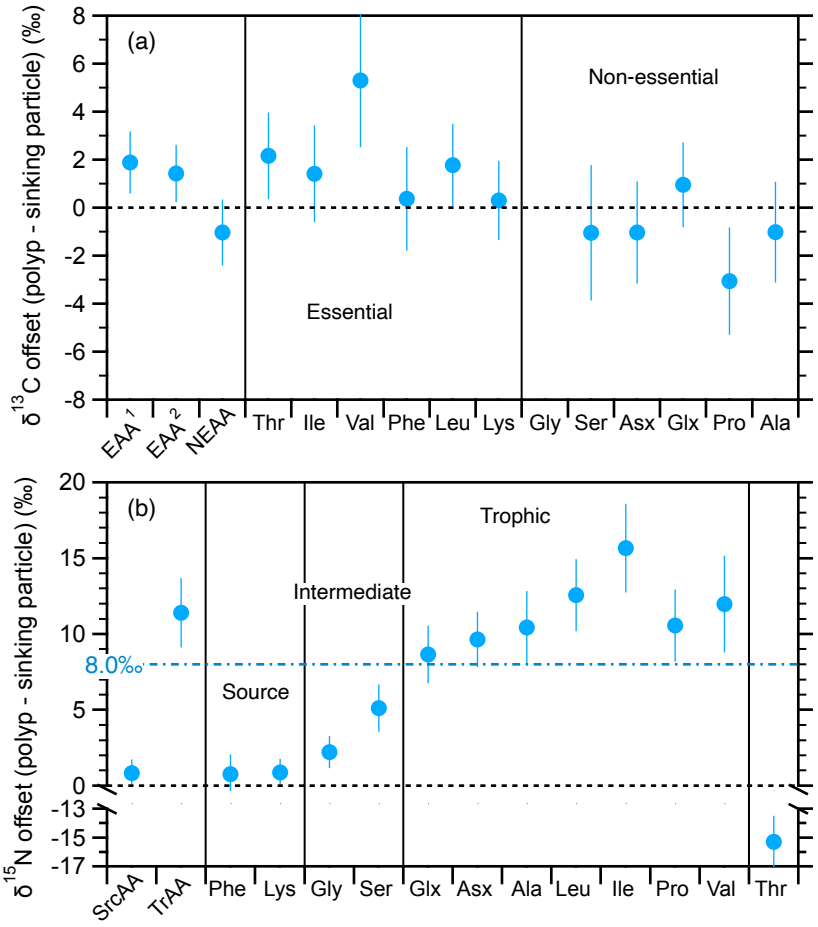

Figure EA4. Corrected offsets (i.e., trophic discrimination factor TDF) in mean $\delta^{13}C$ and $\delta^{15}N$ values of individual amino acids between coral polyp tissues and sinking particles, calculated using correction factors proposed by McMahon and coauthors (2018) for observed fractionation between coral poly tissues and skeletons across three coral species (McMahon et al., 2018). See Equation (7) in the main manuscript. The blue dashed line is the 8.0‰ trophic fractionation of Glx found in zooplankton (Chikaraishi et al., 2009). EAA^1: average $\delta^{13}C$ value of all six essential AAs; EAA^2: average $\delta^{13}C$ value of essential AAs without Val. Error bars represent propagated standard deviations.

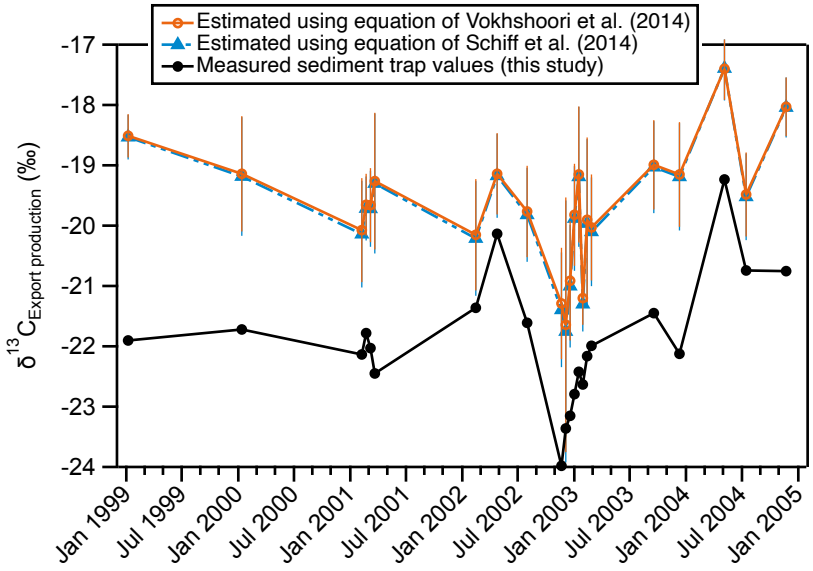

Figure EA5. Comparision of estimated bulk $\delta^{13}C$ values of export production using previously published equations versus our data. The equation of Vokhshoori et al. (2014) was derived from a diverse range of freshwater and marine photoautotrophs, including eukaryotic and prokaryotic species ($\delta^{13}C_{bulk} = 0.9274 \times \delta^{13}C_{EAA} + 0.0769$; $n = 18$). The equation of Schiff et al. (2014) was derived from a modified sample set that included only the eukaryotic diatom and dinoflagellate ($\delta^{13}C_{bulk} = 0.9528 \times \delta^{13}C_{EAA} + 0.5658$; $n = 8$). Measured values from our sediment trap samples are shown in black solid circles as reference records. As described in the text, moderate to large offsets between lab and field-based model estimates demonstrates the importance of parametrizing equations with locally relevant POM data.